
Catalytic reforming of logistic fuels at high-temperatures

Olaf Deutschmann^a

DOI: 10.1039/9781849734776-00048

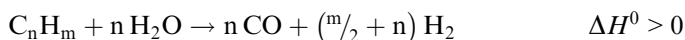
This chapter reviews recent studies of catalytic reforming of logistic fuels at high-temperature. Aside from steam and autothermal reforming, special consideration is given to partial oxidation conditions. Natural gas, gasoline, diesel, and ethanol containing fuels are discussed. Methane and iso-octane as fuel surrogates are exemplarily used to explain the behavior of the reformers in particular focusing on the interaction of heterogeneous and homogeneous chemical reactions and mass and heat transport. As catalyst of choice for reforming, rhodium-based systems are in the focus of this review but alternate catalysts are noted as well.

1 Introduction

Recently a variety of studies has been published with the focus on hydrogen production from logistic transportation fuels by catalytic reforming at high temperatures and short contact times.^{1–10} Compact designs can be realized due to high throughputs making these reformers attractive for on-board supply of hydrogen and reformat fuel from conventional logistic as well as synthetic fuels, which can be integrated into auxiliary power units based on proton exchange membrane (PEMFC) and solid oxide (SOFC) fuel cells.¹¹ Fuels under consideration range from natural gas to all kinds of liquid fuels such as gasoline, diesel, kerosene, ethanol, and ethanol blended fuels. The technical applications however are still facing challenges such as the costs of the catalyst, catalyst deactivation by agglomeration, vaporization, sulfur poisoning, and formation of carbonaceous overlayers, coking downstream the catalyst due to the formation of coke precursors like olefins, problems of thermal and mechanical stability, exhaust gas recycling, heat management, quick start-up and shut-down, control issues, and strong variation in fuel composition.

Therefore, many regimes of operation have been proposed, which can be grouped into three main catalytic reforming reactions to convert hydrocarbon fuels into synthesis gas (H₂ and CO):

Steam reforming (SR):



Partial oxidation (POX):



^aInstitute for Chemical Technology and Polymer Chemistry, Karlsruhe Institute of Technology (KIT), Engesserstr. 20, 76128 Karlsruhe, Germany. E-mail: deutschmann@kit.edu



When the exhaust gas is recycled, the actual stoichiometry of the reaction represents a mixture of those reactions including dry reforming. In the presence of oxygen, total oxidation will always play a certain role, often providing the heat to operate the system autothermally at sufficiently high temperature. The water-gas-shift reaction (WGS) is always present moving the product composition towards the thermodynamic equilibrium between CO, H₂O, H₂ and CO₂. The subsequent production of hydrogen-rich syngas (minimization of CO content), in particular for PEM fuel cell application, is also based on WGS.

In the last two decades, the pioneering work of the Schmidt group at Minnesota led to hundreds of studies, in which basically all gaseous, liquid, and solid hydrocarbon containing fuels, from natural gas to biomass, have been shown to efficiently produce synthesis gas over rhodium based catalysts within a fraction of a second by partial oxidation. Catalytic partial oxidation (CPOX) in these so-called short-contact time reactors can be operated autothermally at temperatures above 1000 K. Short monolithic honeycomb and foam structures made out of metal oxides usually serve as catalyst carrier. Due to the high fuel throughput the reactors are nearly adiabatic; however the small heat release matters to understand the reactor behavior at varying flow rate. Nevertheless, CPOX reactors are the most promising type of reformer for on-board and any other mobile application, in which synthesis gas or hydrogen has to be produced in a compact autothermal system. The reasons for this attractiveness are the facts that no additional energy and water is needed, ambient air can serve as oxygen carrier, and light-off and shut-down handling is relatively straight-forward.

A scheme of potential applications of a CPOX reactor on-board a vehicle is given in Fig. 1. Catalytic partial oxidation of the fuel provides synthesis gas, which can either directly be used in a SOFC or after CO cleaning in a Fuel Processing System (FPS) in a PEM FC, realizing an Auxiliary Power Unit (APU), which provides electricity for on-road and idling loads. Prototypes with up to 3 kW electrical power output were already presented for heavy-duty vehicles.¹² Such applications may significantly decrease the fuel consumption needed for electrical devices on-board, because the efficiencies of the conventional systems are rather poor, in particular in idling load. Aside from that, noise and local pollution emission will be reduced. Furthermore, the syngas produced can be added to the combustion fuel during engine start-up when the exhaust-gas after treatment system has not reached its operation temperature, and hence emissions of hydrocarbons, carbon monoxide, and nitrogen oxides are extraordinary high. Addition of syngas to the fuel has been shown to reduce the primarily emissions of those pollutants. Finally, hydrogen, and even CO can serve as reducing agents for the nitrogen oxides in the exhaust-gas after-treatment system.

Catalytic partial oxidation (CPOX) of natural gas over noble metal catalysts at short contact times offers other promising applications aside from electricity supply. CPOX of natural gas containing also ethane and propane

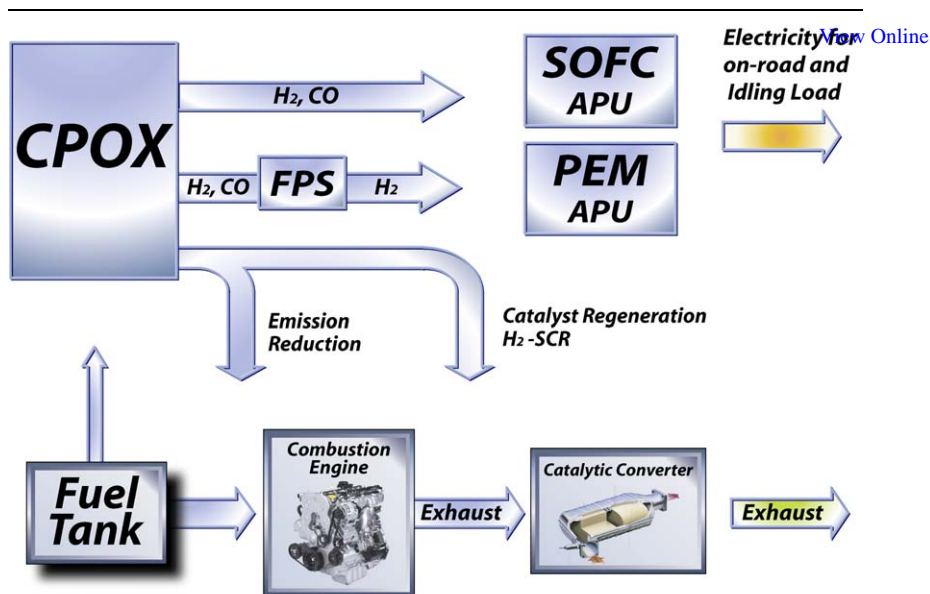


Fig. 1 Scheme of the use of a catalytic partial oxidation (CPOX) reactor on board a vehicle; FPS = fuel processing system, PEMFC = proton exchange membrane fuel cell, SOFC = solid oxide fuel cell, APU = auxiliary power unit, SCR = selective catalytic reduction, taken from reference (O. Deutschmann, *Chemie Ingenieur Technik*, 2011, **83**(11), 1–12).

aside from its main constituent methane cannot only be applied for the production of synthesis gas^{13,14} as a potential basic feedstock for chemical industry but also for the production of olefins^{15,16} as the raw material of most plastics. Furthermore, synthesis gas is the first intermediate in (gas-to-liquids) plants for the production of for instance methanol and synthetic diesel.

Due to the high costs of Rh, substantial work has been conducted to find effective but less expensive alternate catalysts. Since reviewing catalyst developments in the area of fuel reforming is beyond the scope of this chapter, the readers are referred to the literature, for instance to a recent review on catalysts for hydrogen production from heavy hydrocarbons by Navarro Yerga *et al.*¹⁷ and recent work by Spivey *et al.*^{18,19}

This chapter will focus on recent developments in catalytic reforming of logistic fuels such as natural gas, gasoline, diesel, ethanol, and ethanol blended gasoline. Whenever possible, fundamental studies of the reactor behavior towards an understanding of the interaction of chemistry and mass and heat transport in such reactors will be discussed, because only a fundamental understanding will finally lead to proper design of the reformer and an optimization of the operating conditions. Since rhodium still is the catalyst of choice, the discussion will focus on Rh-based catalysts. The chapter will at first discuss the fundamentals of high-temperature catalysis and, then, in the subsequent section, deal with specific transportation and model fuels.

2 Fundamentals of high-temperature catalysis

High-temperature catalysis is not a new concept; the Oswald process for the NO production by oxidation of ammonia over noble metal gauzes at

temperatures above 1000 °C and residence times of less than a micro second has been technically applied for decades; total oxidation of hydrogen and methane (catalytic combustion) over platinum catalysts were even used before Berzelius proposed the term “catalysis”. Recently, however, high-temperature catalysis has been extensively discussed again, in particular in the light of the synthesis of basic chemicals and hydrogen, and high-temperature fuel cells. This section focuses on the fundamentals of heterogeneously catalyzed gas-phase reactions and their interaction with the surrounding flow field in high-temperature catalysis. Understanding and optimization of heterogeneous reactive systems require the knowledge of the physical and chemical processes on a molecular level. In particular, at short contact times and high temperatures reactions occur on the catalyst and in the gas-phase and the interactions of transport and chemistry become important.

Monolithic reactors can serve as an example, which are frequently used not only for partial oxidation, steam reforming, and autothermal reforming of hydrocarbon fuels but even more for the reduction of pollutant emissions from automobiles. Fig. 2 illustrates the physical and chemical processes in a high-temperature catalytic monolith that glows at a temperature of around 1000 °C due to the exothermic oxidation reactions. In each channel of the monolith, the transport of momentum, energy, and chemical species occurs not only in flow (axial) direction, but also in radial direction. The reactants diffuse to the inner channel wall, which is coated with the catalytic material, where the gaseous species adsorb and react on the surface. The products and intermediates desorb and diffuse back into the bulk flow. Due to the high temperatures, the chemical species may also react homogeneously in the gas phase. In catalytic reactors, the catalyst material is often dispersed in porous structures like washcoats or pellets. Mass transport in the fluid phase and chemical reactions are then superimposed by diffusion

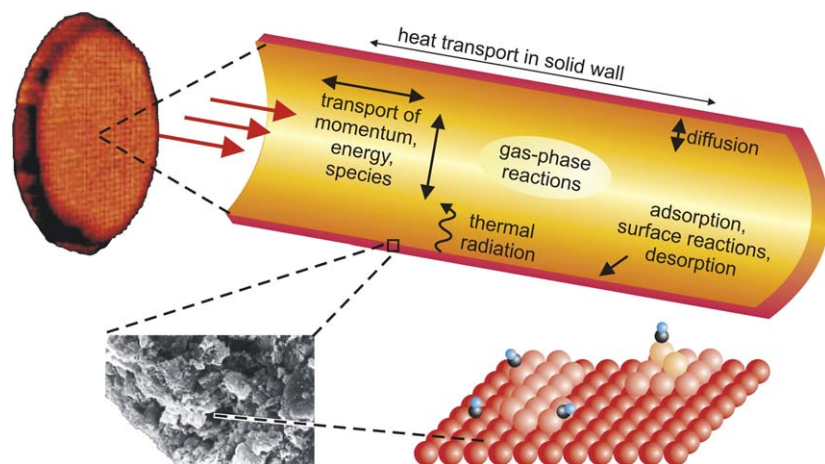


Fig. 2 Catalytic combustion monolith and physical and chemical processes occurring in a single monolith channel. Many lengths and time scales have to be considered simultaneously reaching from the nanometer and picosecond scale (*e.g.* surface reactions) via the micro/millimeter and micro/millisecond scale (*e.g.* internal/external diffusion) to the centimeter and second scale (*e.g.* heat transport in solid structures), taken from reference (O. Deutschmann, *Chemie Ingenieur Technik*, 2011, **83**(11), 1–12).

of the species to the active catalytic centers in the pores. The temperature distribution depends on the interaction of heat convection and conduction in the fluid, heat generation due to chemical reactions, heat transport in the solid material, and thermal radiation. Both variation of the feed conditions in time and space and heat transfer between the reactor and the ambience result in a non-uniform temperature distribution over the entire monolith, which means that the behavior will differ from channel to channel.²⁰

Today, the challenge in catalysis is not only the development of new catalysts to synthesize a desired product, but also the understanding of the interaction of the catalyst with the surrounding reactive flow field. Sometimes, only the use of these interactions can lead to the desired product selectivity and yield. For detailed introductions into transport phenomena and their coupling with heterogeneous reactions the readers are referred to references 21–25 and 25, 26 respectively.

In the remainder of this section 2, the individual physical and chemical processes and their coupling will be discussed beginning with the reactions of the solid catalyst.

2.1 Heterogeneous reaction mechanisms

The understanding of the catalytic cycle in fuel reformers is a crucial step in reformer design and optimization. The development of a reliable surface reaction mechanism is a complex process, today increasingly based on the elucidation of the molecular steps. A survey on state-of-the-art modeling of heterogeneously catalyzed gas-phase reactions can be found, *e.g.*, in reference 27. The most frequent approach for modeling reaction mechanisms and calculating reaction rates in technical systems is the mean-field approximation.²⁶ In this approach, a tentative reaction mechanism is proposed based on experimental surface science studies, on analogy to gas-phase kinetics and organo-metallic compounds, and on theoretical studies, increasingly including DFT and Monte-Carlo simulations. This mechanism should include all possible paths for the formation of the chemical species under consideration in order to be “elementary-like” and thus applicable over a wide range of conditions. The mechanism idea then needs to be evaluated by numerous experimentally derived data, which are compared with theoretical predictions based on the mechanism. Here, the simulations of the laboratory reactors require appropriate models for all significant processes in order to evaluate the intrinsic kinetics. Sensitivity analysis leads to the crucial steps in the mechanism, for which refined kinetic experiments and data may be needed.

Since the early nineties, many groups have developed surface reaction mechanisms for high-temperature catalysis, following this concept, which has been adapted from modeling homogeneous gas-phase reactions in particular in the fields of combustion²³ and pyrolysis²⁸ of hydrocarbons. Consequently, this concept becomes handy when high-temperature processes in catalysis are considered, in particular when the radical interactions between the solid phase (catalyst) and the surrounding gas-phase (fluid flow) have an impact on the overall rate.

In this concept, the surface reaction rate is related to the size of the computational cell in the flow field simulation, assuming that the local state of the active surface can be represented by mean values for this cell.

Hence, this model assumes randomly distributed adsorbates. The state of the catalytic surface is described by the temperature T and a set of surface coverages θ_i . The surface temperature and the coverages depend on time and the macroscopic position in the reactor, but are averaged over microscopic local fluctuations.

Since the reactor temperature and concentrations of gaseous species depend on the local position in the reactor, the set of surface coverages also varies with position. However, no lateral interaction of the surface species between different locations on the catalytic surface is modeled. This assumption is justified by the fact that the computational cells in reactor simulations are usually much larger than the range of lateral interactions of the surface processes.

Since the binding states of adsorption of all species vary with the surface coverage, the expression for the rate coefficient is commonly extended by coverage-dependent parameters.^{25,29} A crucial issue with many of the surface mechanisms published is thermodynamic in-consistency.²⁶ Lately, optimization procedures enforcing overall thermodynamic consistency have been applied to overcome this problem.^{30,31}

In particular oxidation reactions, in which radical interactions play a very significant role, have been modeled extensively using the mean-field approach. Examples are the oxidation of hydrogen,^{32–38} CO,^{39–41} methane^{42–47} and ethane^{16,48–50} over Pt, formation of synthesis gas over Rh from different hydrocarbons.^{5,47,51–53} Adsorption and desorption of radicals are often included in the mechanism. These reactions of intermediately formed species are significant not only for the heterogeneous reaction but also for homogeneous conversion in the surrounding fluid. In most cases, the catalyst acts as sink for radicals produced in the gas-phase, and hence radical adsorption slows down or even inhibits gas-phase reaction rates. The interaction between homogeneous and heterogeneous reactions in high-temperature catalysis is still not well-understood; a recent experimental study by the Beretta group for instance reveals that significant amounts of olefins even occur in the fluid phase of tiny catalytic channels.⁵⁴

2.2 Homogeneous reactions

In many catalytic fuel reformers operated at high-temperature, the reactions do not exclusively occur on the catalyst surface but also in the fluid flow. In some reactors even the desired products are mainly produced in the gas phase, for instance in the oxidative dehydrogenation of paraffins to olefins over noble metals at short contact times and high temperature.^{16,50,55–60} Such cases are dominated by the interaction between gas-phase and surface kinetics and transport. One can roughly say whenever C_{2+} species are involved in high-temperature reforming, significant conversion in the gas-phase can occur even at atmospheric pressure. In case of methane reforming, gas-phase reactions can be neglected at pressures up to 10 bar but not above. Therefore, any high-temperature-reactor simulation should include an appropriate model for the homogeneous kinetics along with the flow models. Various reliable sets of elementary reactions are available for modeling homogeneous gas phase reactions, for instance for total²³ and partial oxidation, and pyrolysis of hydrocarbons. In a recent study,

Maier *et al.* compared four detailed gas-phase reaction mechanisms concerning their ability to predict homogeneous fuel conversion in CPOX of iso-octane and found qualitative but not quantitative agreement between modeling and experimentally determined conversion.¹⁰

2.3 Coupling of chemistry and mass and heat transport

The chemical processes at the surface can be coupled with the surrounding flow field by boundary conditions for the species-continuity equations at the gas-surface interface.^{25,29} The calculation of the diffusive flux at the gas-surface interface due to adsorption and desorption of reactants and products, respectively, requires knowledge of the amount of catalytically active surface area in addition to the geometric surface area, which generally has to be determined experimentally, *e.g.* by chemisorption measurements. The effect of internal mass transfer resistance for catalyst dispersed in the usually applied porous washcoat can be included by an effectiveness factor.^{24,61} However, more accurate models such as the Dusty-Gas-Model need to be applied often for an accurate description of the local reaction rate. For more detailed models for transport in porous media the readers are referred to the literature.^{25,62–65}

Even though the implementation of elementary-reaction mechanisms in fluid flow models is straight forward, an additional highly nonlinear coupling is introduced into the governing equations leading to considerable computational efforts. The nonlinearity, the very large number (thousands) of chemical species occurring in reforming of logistic fuels and even in fuel surrogates, and the fact that chemical reactions exhibit a large range of time scales, in particular when radicals are involved, render the solving of those equation systems challenging. In particular for turbulent flows, but sometimes even for laminar flows, the solution of the system is too CPU time-consuming with current numerical algorithms and computer capacities. This calls for the application of reduction algorithms for large reaction mechanisms, for instance, by the extraction of the intrinsic low dimensional manifolds of trajectories in chemical space,⁶⁷ which can be applied for heterogeneous reactions.⁶⁸ Another approach is to use “as little chemistry as necessary”. In these so-called adaptive chemistry methods, the construction of the reaction mechanism includes only steps relevant for the application studied.⁶⁹

2.4 Modeling monolithic catalysts

As an example¹⁰ of modeling a high-temperature catalyst, catalyst coated monolithic structures as given in Fig. 2 are discussed. An efficient approach, which still includes all fundamental aspects, is often used for modeling catalytic monoliths, which is based on the combination of simulations of a representative number of channels with the simulation of the temperature profiles of the solid structure treating the latter one as continuum.^{70,71} This approach has for instance been implemented in the computer code DETCHEM^{MONOLITH},⁶⁶ which has frequently been applied to model the transient behavior of catalytic monoliths. The code combines a transient three-dimensional simulation of a catalytic monolith with a 2D model of the single-channel flow field based on the boundary layer

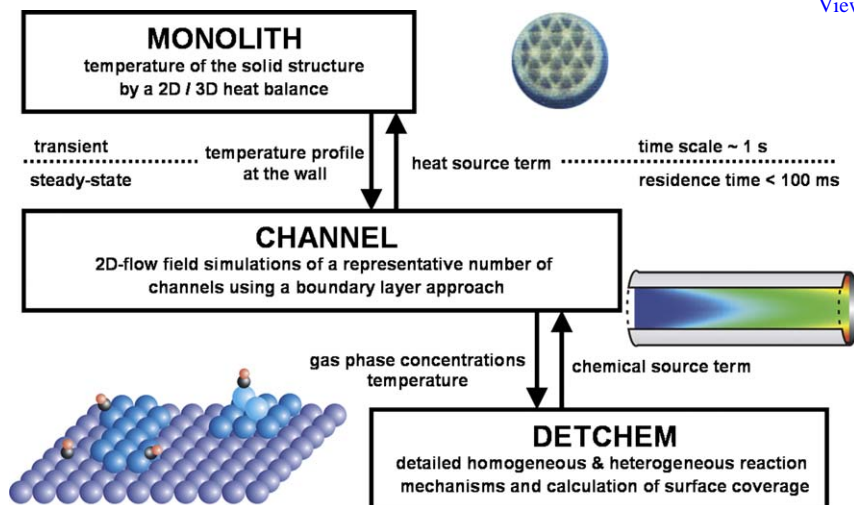


Fig. 3 Structure of the code DETCHEM^{MONOLITH.66}

approximation. It uses detailed models for homogeneous gas-phase chemistry, heterogeneous surface chemistry, and contains a model for the description of pore diffusion in washcoats.

The numerical procedure as sketched in Fig. 3 is based on the following ideas: The residence time of the reactive gas in the monolith channels is much smaller than the unsteadiness of the inlet conditions (temperature, mass flow rate, composition) and the time of significant temperature variations of the solid monolith structure. In high-temperature catalysis the gas residence time is usually on the order of milliseconds, while the inlet conditions and the temperature of the solid vary on the order of seconds. Under these assumptions, the time scales of the channel flow are decoupled from the temporal temperature variations of the solid, and the following procedure can be applied: A transient multi-dimensional heat balance is solved for the monolithic structure including the thermal insulation and reactor walls, which are treated as porous continuum. This simulation of the heat balance provides the temperature profiles along the channel walls. At each time step the reactive flow through a representative number of single channels is simulated including detailed transport and chemistry models. These single-channel simulations also calculate the heat flux from the fluid flow to the channel wall due to convective and conductive heat transport in the gaseous flow and heat released by chemical reactions. Thus, at each time step, the single-channel simulations provide the source terms for the heat balance of the monolith structure while the simulation of the heat balance provides the boundary condition (wall temperature) for the single-channel simulations. At each time step, the inlet conditions may vary. This very efficient iterative procedure enables a transient simulation of the entire monolith without sacrificing the details of the transport and chemistry models, as long as the prerequisites for the time scales remain valid.⁷⁰ Furthermore, reactors with alternating channel properties such as flow directions, catalyst materials, and loadings can be treated.

2.5 *In-situ* experimental studies of high-temperature catalysis

The coupling of several complex models introduces a large number of parameters into the simulations. Hence, agreement between predicted and experimentally observed overall conversion and selectivity alone is not sufficient to evaluate individual sub models. Time and locally resolved profiles provide a more stringent test for model evaluation. Recently, tremendous progress has been made in the application of *in-situ* techniques to determine spatially resolved species and temperature profiles in high-temperature catalytic reactors.

Useful data arise from the experimental resolution of local spatial and temporal species profiles by *in situ*, non-invasive methods such as Raman and laser induced fluorescence (LIF) spectroscopy. For instance, an optically accessible catalytic channel reactor is used in the Mantzaras group (PSI, Switzerland) to evaluate models for heterogeneous and homogeneous chemistry as well as transport relevant for fuel reforming by the simultaneous detection of stable species by Raman measurements and OH radicals by Planar laser-induced fluorescence (PLIF).^{72–78} This technique was for instance applied to resolve the axial and radial profiles in catalytic partial oxidation with exhaust gas recycling of methane at elevated pressure as shown in Fig. 4.^{75,79}

The Horn group (FHI, Berlin) has recently developed an *in-situ* sampling capillary technique for measurements of spatially resolved profiles in reforming catalytic foams up to 1300 °C and 45 bar and applied this technique to elucidate axial profiles in partial oxidation of methane over noble metal catalyst as shown in Fig. 5.⁸⁰

The Beretta group (Politecnico di Milano) also developed a quartz capillary sampling system to spatially resolve the gas-phase composition in monolithic catalysts, which was recently applied to find olefins in the initial catalyst section over a Rh/alumina catalysts in CPOX of propane.⁵⁴

2.6 Mathematical optimization of reformer design and operating conditions

In reforming reactors, the C/O ratio, steam addition, exhaust recycling, temperature, pressure and residence time can be used to optimize conversion and selectivity and to avoid formation of harmful by-products. Furthermore, the catalyst loading along the channel can be varied or even different active components and washcoat structures may be used. Recently, a new mathematical algorithm was developed to not only optimize the operating conditions but also the catalyst loading.^{81–83} These new computational tools were recently applied to optimize catalytic oxy-dehydrogenation of ethane at high temperatures and short contact times by Minh *et al.*⁸¹ In their study, radical interactions in gas and surface chemistry were shown to play a decisive role for yield increase. These tools may support design and operation of catalytic fuel reformers in the near future.

3 Reforming of natural gas

Synthesis gas (H₂/CO in various compositions) plays a key role as a feedstock in many catalytic processes such as synthesis of methanol, oxo-synthesis, and

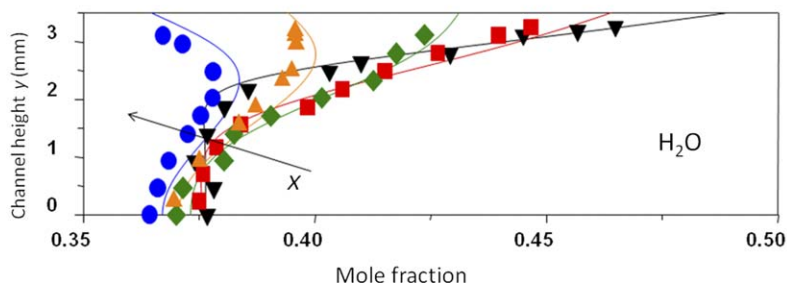
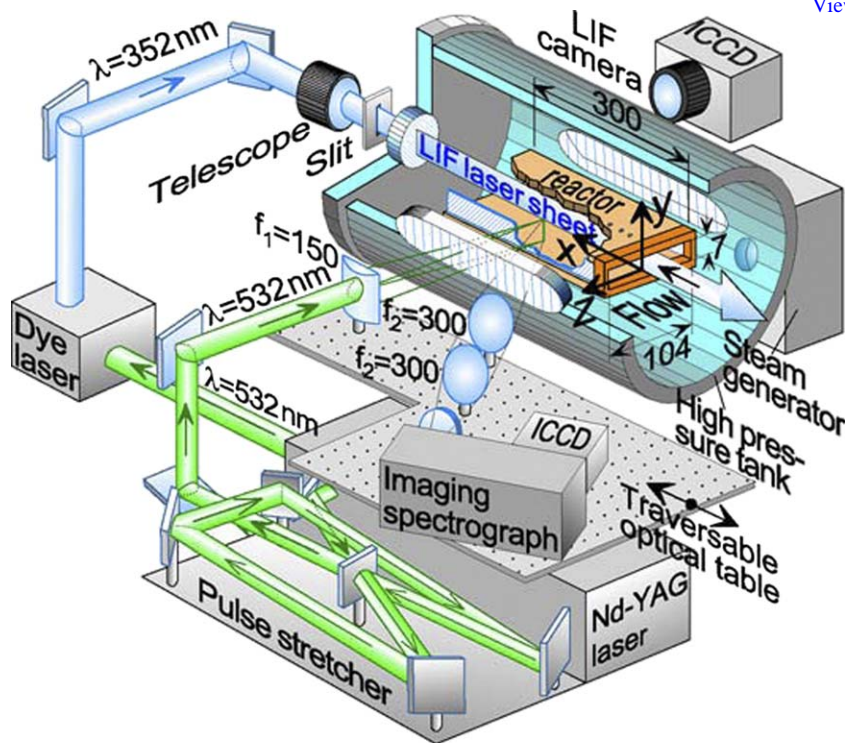


Fig. 4 Schematic of the reactor and the Raman/LIF set-up (top) of Mantzaras *et al.*⁷⁸ to study spatial profiles in high-temperature catalysis. Predicted (lines) and measured (symbols) steam profiles for autothermal reforming of methane over Rh at 6 bar, equivalence ratio of 4, and 38% steam addition, adapted from Schneider *et al.*⁷⁵ The profiles are given at different axial positions of $x=2$ (black triangle), 5 (red square), 9 (green diamond), 13 (orange triangle), 17 (blue sphere) cm; the arrow denotes the flow direction (x); catalytic wall at $y=3.5$ mm, channel centerline at $y=0$.

Fischer-Tropsch synthesis. Hydrogen as a separate component of synthesis gas is largely used in the manufacturing of ammonia, in a variety of petroleum hydrogenation processes, and as a clean fuel for burners or fuel cells. In future, we will likely see a steep increase in the use of natural gas as primary fuel for stationary and mobile fuel cell applications for the generation of electricity. For this, but also for the conventional purposes of natural gas reforming, the interest in autothermally operated reformers for the conversion of natural gas into synthesis gas and hydrogen will grow further.

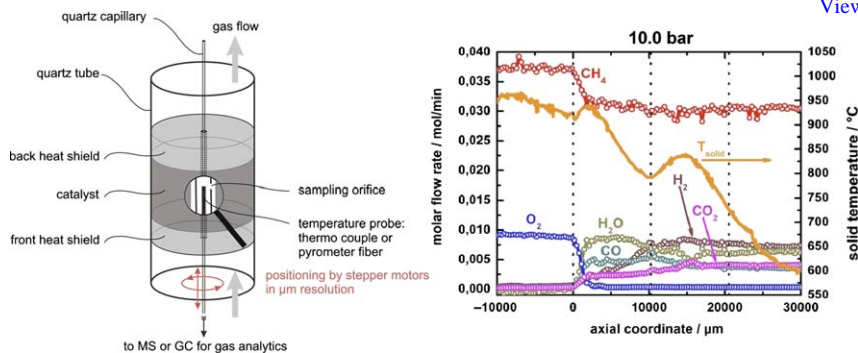


Fig. 5 Principle of spatially resolved measurements in foam catalyst (left) and spatial profiles for autothermal methane oxidation on 0.6 wt % Pt coated 45 ppi/alumina foam catalysts. Gas flow: 911 ml min⁻¹ CH₄, 228 ml min⁻¹ O₂, 858 ml min⁻¹ Ar, C/O = 2.0 (right), taken from Horn *et al.*⁸⁰

So far, steam reforming of natural gas has been the most widely used industrial process, because it is one of the most efficient technologies for hydrogen and the synthesis gas production from fossil fuels in large scale facilities reaching yields close to the thermodynamic equilibrium.⁸⁴ Steam reforming is a highly endothermic reaction and requires an efficient external energy supply, disadvantageous in small scale operation units. Conventional steam reformers deliver relatively high concentrations of hydrogen at high fuel conversion. The molar steam/carbon (S/C) ratio usually exceeds 2.5. The excess steam supports completion of the reaction and inhibits coke formation, however, additional heat must be added.⁸⁵ The products of the reaction are controlled mainly by thermodynamics, which favour the formation of methane at lower temperatures and of hydrogen at higher ones. Recently, direct synthesis of Ni based hydrotalcite was used to prepare small Ni nanocrystals, which can efficiently be applied for sorption enhanced steam methane reforming.⁸⁶

In recent years, (catalytic) partial oxidation ((C)POX),^{51,87–92} in particular over noble metal catalysts and at short contact times due to the pioneering work of the Schmidt group (U Minnesota), as well as CO₂ reforming of natural gas to synthesis gas have also attracted much interest because of their potential to reduce the cost of synthesis gas production and environmental concerns, respectively. Autothermal reforming does not require external energy supplies. Dry reforming (DR) using CO₂ is especially discussed in the light of the useful processing of a greenhouse gas in the chemical industry. The energy and steam produced by the exothermic oxidation reactions in ATR sustain the endothermic reforming reactions to autothermally operate the reactor.

3.1 Mechanistic aspects of reforming of methane over Rh and Ni catalysts

For reaching a profound understanding of the reaction mechanism of synthesis gas formation from methane by SR and POX, the sequence and interaction of the reaction routes have to be analyzed for the combined

POX-SR-DR systems, because the conditions in any flow reactor vary along the flow directions, covering a wide range of mixture compositions and leading to quite different local reaction rates. In CPOX over the commonly used Rh catalysts, the general consensus is now that the overall conversion is realized in a quasi two-step process (indirect route), in which first CH₄ is totally oxidized to CO₂ and steam, as long as oxygen is present close to the catalyst surface, and then the remaining CH₄ is reformed with steam and (or) CO₂ to synthesis gas.^{51,80,91} A decade ago, a direct CPOX route had also been considered. Detailed reaction schemes for the catalytic partial oxidation of methane over platinum and rhodium, which also include steps for steam reforming, were published by Schmidt *et al.*,⁹³ Vlachos *et al.*^{30,94–96} and Deutschmann *et al.*^{42,51,97,98} A unified mechanism covering all aspects of steam and dry reforming, partial and total oxidation, carbon formation, and catalyst oxidation is still under construction. New experimental data as recently obtained for dry-reforming⁹⁹ call for further adaption of the kinetic schemes available.

The development of a detailed mechanism for simultaneous modeling of partial oxidation and steam reforming over nickel catalysts has not been described yet, even though reaction kinetics of methane steam reforming over nickel catalysts has been extensively investigated experimentally and theoretically.^{100–104} A review on catalytic partial oxidation of methane to synthesis gas with emphasis on reaction mechanisms over transition metal catalysts was recently published by Holmen and co-workers.¹⁰⁵ A hierarchical, multiscale modeling approach was recently demonstrated by Chen *et al.*¹⁰⁶ including a microkinetic model for steam methane reforming on the supported Ni catalyst including reaction steps of surface carbon formation, segregation, diffusion, and precipitation. A mechanism recently developed for Ni/alumina catalysts³¹ was also successfully applied in numerical simulation of internal steam and dry reforming of methane over Ni/YSZ anodes of solid-oxide fuel cells (SOFC).^{52,107}

3.2 Interaction of surface reactions and mass and heat transport

Autothermal catalytic reforming of natural gas has been studied very extensively over the last decades. The high-temperature catalytic partial oxidation (CPOX) of methane over Rh based catalysts in short contact time (milliseconds) reactors has been intensively studied, because it offers a promising route to convert natural gas into synthesis gas and hydrogen, which can subsequently be converted to higher alkanes or methanol and be used in fuel cells, respectively.^{13,92,108} The indirect route for syngas formation has meanwhile been accepted, which can also be recognized by the experimental data given in Figs. 4 and 5. At the catalyst entrance total oxidation occurs to form steam as long as oxygen is available at the surface, then methane is steam-reformed to hydrogen. Basically no dry reforming occurs and the surface acts as sink for radicals inhibiting significant gas-phase reactions at pressures below 10 bar.⁹⁸ Also, the transient behavior during light-off of the reaction has been revealed. Exemplarily, Fig. 6 shows the time-resolved temperature and species profiles in a single channel of a catalytic monolith for partial oxidation of methane for the production

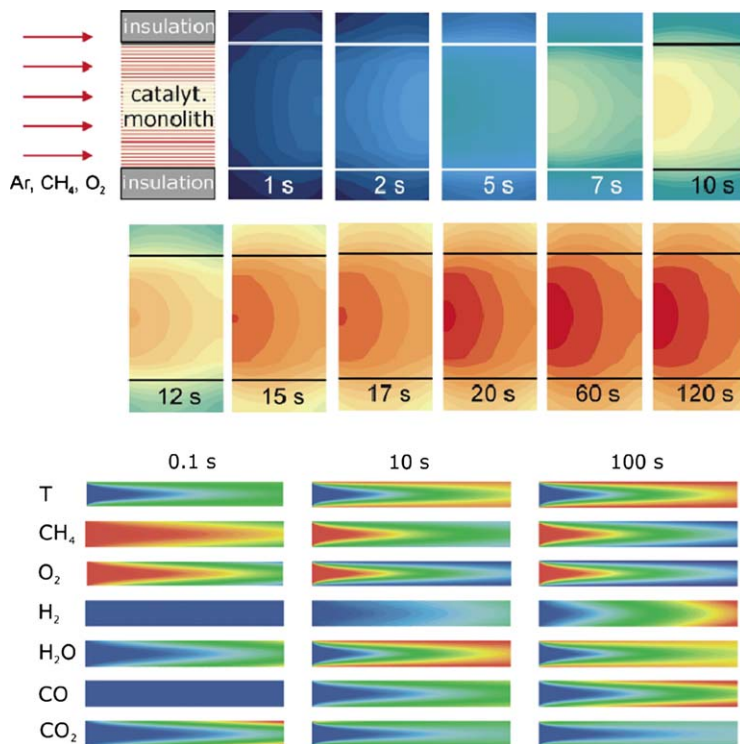


Fig. 6 Numerical simulation of the light-off of a Rh/Al₂O₃ coated monolithic honeycomb reactor coated for partial oxidation of methane to synthesis gas.⁵¹ Top panel: temperature of the solid structure of the catalytic monolith and the thermal insulation (675 K (blue) to 925 K (red)). Lower panel: gas-phase temperature (385–900 K), and species mole fractions (CH₄: 0.043–0.094, O₂: 0–0.055, H₂: 0–0.0412, H₂O: 0–0.058, CO: 0–0.042, CO₂: 0–0.056) in a single channel in the center of the monolith, red = maximum, blue = minimum. The time is set to zero when significant amounts of products can be observed after the reactor was heated up to the ignition temperature of 675 K.

of synthesis gas and the temperature distribution of the solid structure during light-off.⁵¹

Since natural gas contains higher alkanes and other minor components besides methane, conversion and selectivity can be influenced by those other components. Consequently, conversion of methane in steam reforming of pure methane and in steam reforming of natural gas (North Sea H) differ.^{109,110} Before substantial conversion of methane sets in, most of the heavier hydrocarbons are fully converted.

4 Reforming of gasoline fuels

The production of hydrogen and synthesis gas from gasoline by catalytic partial oxidation (CPOX) and steam reforming (SR) is currently in the focus of both academic and industrial research. In contrast to the complex and costly supply of compressed and stored hydrogen for mobile fuel cell application, CPOX of liquid fuels allows production and utilization of hydrogen through existing routes, which, in particular, is of interest for on-board applications. At operating temperatures around 1000 K and

higher, conversion of the fuel may not only occur on the solid catalyst but also in the gas-phase. This behaviour is very different from reforming of methane. Heterogeneous and homogeneous reactions in CPOX of all higher (C_{2+}) hydrocarbons are coupled not only by adsorption and desorption of fuel and oxygen molecules and the products, respectively, but also by adsorption and desorption of intermediates and radicals. Therefore, mass transport of radicals and intermediates from/to the gaseous bulk phase and the catalytically active channel wall, mainly by radial diffusion in the small channels of the monolith being on the order of a quarter to one millimeter, is crucial for the interaction of heterogeneous and homogeneous reactions in CPOX reactors.

In technical systems overall efficiency is increased by heat integration, which can be realized either indirectly or directly. For the first case, Fig. 7 shows the scheme of a potential technical application, in which the hot exhaust of the SOFC stack at approximately $800\text{ }^{\circ}\text{C}$ is led through the housing of the reformer to improve the heat balance.¹¹¹ In case part of the exhaust is directly co-fed to the fuel/air mixture, one has to be aware of the fact that the oxygen contained in steam and in particular in carbon dioxide may show different reactivity than the oxygen of O_2 .

The varying composition of gasoline fuels challenges any model predictions of the performance of catalytic gasoline reformers. The composition does not only influence the overall hydrogen yield but also the propensity of the coke formation. A systematic study on reforming of gasoline

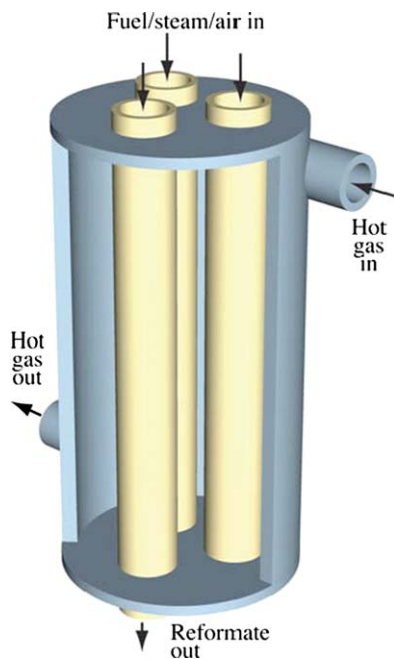


Fig. 7 Illustration of a shell-and-tube reformer. Catalytic reforming proceeds within the tubes, with the outer shell flow (exhaust gas recycle) used to assist control of the tube temperatures; taken from Goldin *et al.*¹¹¹

components over Rh/Al₂O₃ coated monoliths for a wide range of C/O ratios was recently conducted by Hartmann *et al.*¹¹² [View Online](#)

4.1 Reactivity of individual gasoline components in CPOX over Rh/Al₂O₃

In a well-defined flow reactor with FTIR, GC, and MS analytics,¹¹³ Hartmann *et al.* studied the autothermally operated catalytic partial oxidation of higher hydrocarbon fuel components on Rh/Al₂O₃ coated honeycomb monoliths at short residence times.¹¹² Fig. 8 gives a sketch of the reactor system, in which fuels with boiling points up to 280 °C mixed with synthetic air can be fed to the monoliths with a homogeneous, pulse-free reactant flow and uniform (over the tube cross section) temperature profile. The catalytic monolith is made out of cordierite, 1 cm in length and 1.9 cm in diameter with a cell density of 600 cpsi. The inner channel walls are coated with rhodium (4.23 mg/cm³) dispersed on a γ -alumina washcoat; no further additives are used. The catalyst is positioned 20 cm downstream the mixture inlet. Upstream and downstream the catalyst, uncoated foam and honeycomb monoliths, respectively, are placed close to the catalyst as flow homogenizers, heat shields, and fixations for thermocouples. The reactants are fed to the catalyst with 80 % dilution in nitrogen at 190 °C at a space velocity of 85.000 h⁻¹. For the initial preheating, the reactor is placed in a furnace, which is switched-off after ignition.

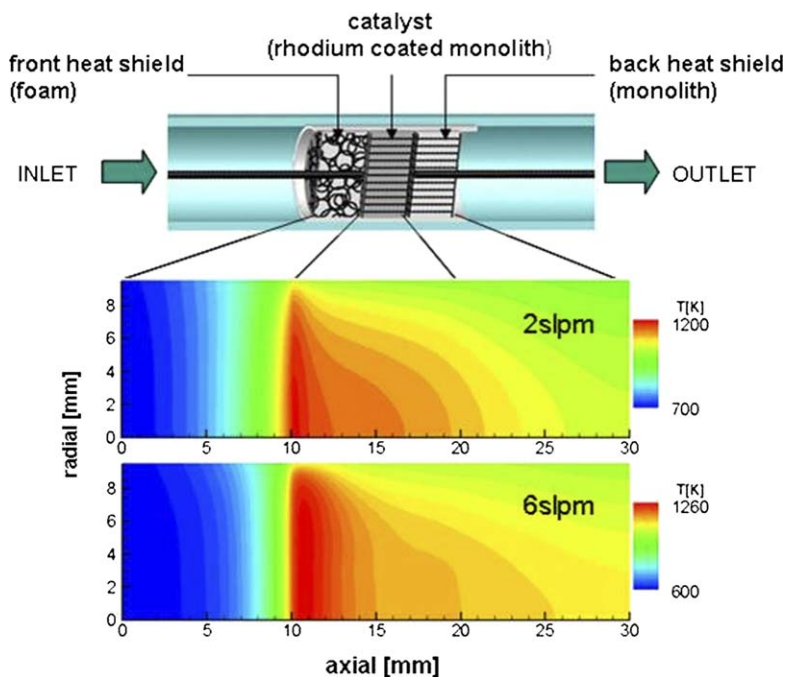


Fig. 8 Sketch of the catalyst section of a reformer for logistic fuels with two heat shields (top) and numerically predicted steady-state monolith temperature at C/O = 1.0 and at flow rates of 2 slpm (middle) and 6 slpm (bottom) in CPOX of iso-octane over a Rh/alumina coated honeycomb monolith. The symmetry axis of the monolith is at radial dimension of zero. Taken from Maier *et al.*¹⁰

The impact of the chemical structure and chain length of hydrocarbons in CPOX over Rh based catalysts has been studied using benzene, cyclohexane, 1-hexene, and i-hexane (3-methylpentane) for the representation of archetypical constituents of logistic fuels.¹¹² Since these species have the same number of carbon atoms, their performance can easily be compared using the molar carbon-to-oxygen (C/O) ratio. The influence of the fuel components is studied by comparison of a series of linear alkanes ranging from n-hexane to n-dodecane, representing the wide range of boiling points of the individual fuel components. Furthermore, the effect of side chains of cyclic hydrocarbons has been studied by using species with methyl substitution of benzene and cyclohexane.

This study revealed the dominant role of the structure of the hydrocarbon fuel (n alkanes, i-alkanes, cycloalkanes, olefins or aromatics) on the production of synthesis gas as well as cracking products as shown in Figs. 9 and 10. Especially the presence of double bonds or an aromatic ring shifts

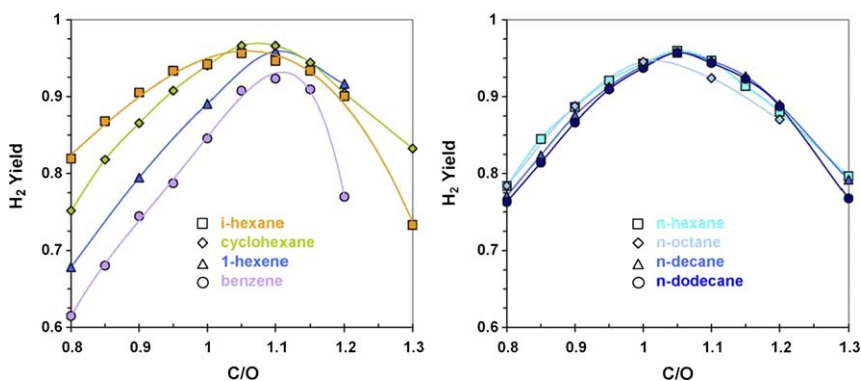


Fig. 9 H₂ yields in CPOX of characteristic components of logistic transportation fuels over Rh/alumina-coated honeycomb catalysts as function of C/O ratio; taken from Hartmann *et al.*¹¹²

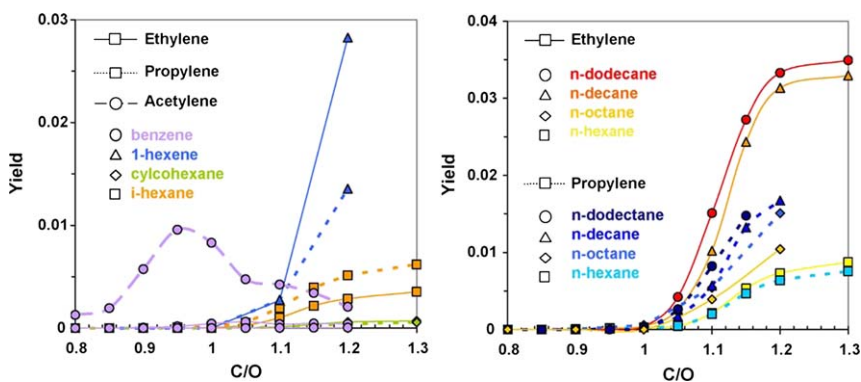


Fig. 10 C based yields of unsaturated hydrocarbons produced by thermal cracking of different C₆ hydrocarbons (left) and n-alkanes (right) in CPOX of characteristic components of logistic transportation fuels over Rh-based catalysts as function of C/O ratio; taken from Hartmann *et al.*¹¹²

the yield to total oxidation products (not directly shown in Figs. 9 and 10).¹¹² On the other side, over a wide range of boiling points, equivalent performance is observed for varying chain length of the hydrocarbon backbone or the appearance of side chains. Only a minor variation of the distribution of products can be observed by the addition of a methyl group to *c*-hexane.

In particular ethylene, propylene, and acetylene represent precursors for coke formation in reforming processes.^{114–116} The propensity of the formation of such coke precursors is also dominated by the structure of the hydrocarbon fuel as shown in Fig. 10.¹¹² Acetylene is exclusively found in conversion of aromatic hydrocarbons. Furthermore, acetylene is the only hydrocarbon cracking product formed under fuel lean conditions, which can be dedicated to the high reaction temperatures reached in conversion of aromatic hydrocarbon fuels and by an excess of oxygen. Ethylene production is observed at $C/O > 1.0$ as further coupling product with concentrations of approximately 50 ppm. The strong increase in formation of α -olefins with increasing C/O in CPOX of hydrocarbons has already been discussed in several papers by Schmidt *et al.*⁵⁹

Based upon the knowledge of the reaction of characteristic fuel constituents, surrogates of logistic fuels can be derived. Besides the reduction of the high complexity of commercial fuels in model fuels, the use of surrogates allows a reliable standardization and reproduction of CPOX experiments. Moreover, the influence and interaction of dominant constituents can be explored, allowing the development of detailed models for CPOX of logistic fuels.

4.2 Kinetic aspects of high-temperature reforming of iso-octane over Rh catalysts

In comparison to autothermal reforming of natural gas, the kinetics of reforming of higher hydrocarbons is much more challenging not only due to the fact that the catalytic reaction cycle becomes very complex but also due to the fact that conversion in the gas-phase cannot be neglected any more. In particular, the formation of coke precursors is expected to occur in the gas-phase. For a better understanding of the interactions of surface and gas-phase reactions as well as mass transport (radial diffusion), a fundamental study was conducted using iso-octane as fuel surrogate and focussing on the process in a single channel.⁵³

Using the experimental set-up described above,^{112,113} catalytic partial oxidation of iso-octane over a rhodium/alumina coated honeycomb monolith was studied at varying C/O ratio. Very high hydrogen and carbon monoxide selectivity were found at stoichiometric conditions ($C/O = 1$), while at lean conditions more total oxidation occurs. At rich conditions ($C/O > 1$), homogeneous chemical conversion in the gas-phase is responsible for the formation of by-products such as olefins shown in Fig. 11.

In a first modeling approach of CPOX of iso-octane in this system, a single channel of the monolith at isothermal conditions was numerically simulated using a two-dimensional parabolic flow field description¹¹⁷ coupled with elementary-step based heterogeneous and homogeneous reaction mechanisms (software DETCHEM^{CHANNEL}, refs. 66, 71).

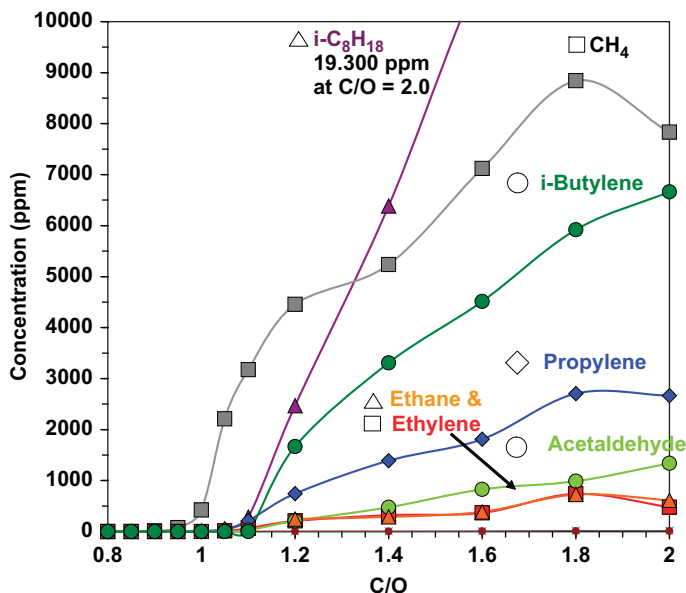


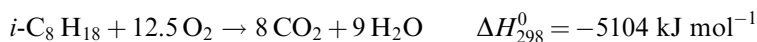
Fig. 11 Experimentally determined concentrations of the side products and the fuel remaining in the outlet stream in CPOX of *i*-octane over a Rh/alumina coated honeycomb monolith as a function of C/O ratio, taken from reference 53.

The chemical models need to be able to predict all macrokinetic features of the chemistry, which are expressed by the following global reactions:

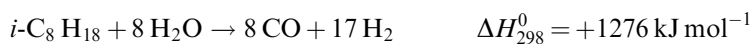
direct partial oxidation



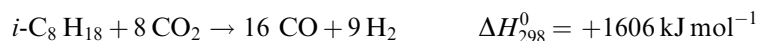
total oxidation



steam reforming



dry reforming



water-gas shift reaction



methanation



Boudouard reaction



Even though it is possible to fit a set of experimental data using the sufficiently large number of adjustable kinetic parameters in this global

reaction scheme, little insight can be gained from such a lumped mechanism. Therefore, it is recommended to apply chemical models based on elementary-step reaction mechanisms. Since the actual decomposition of adsorbed iso-octane over Rh is not known in detail, a simplified approach was proposed: The heterogeneous partial oxidation of i-octane on rhodium-based catalysts is modeled by a detailed surface reaction mechanism for partial oxidation of C₁-C₃ species,⁵³ consisting of 56 reactions and 17 adsorbed species. This scheme is extended by two additional “lumped” reactions for adsorption of iso-octane assuming that iso-octane adsorption quickly leads to the species that are explicitly described in the mechanism.

Conversion may not only occur on the catalytic surface but also in the gas phase due to the high operating temperatures. Several detailed schemes for oxidation and pyrolysis of higher alkanes have been proposed. In the study of Maier *et al.*⁵³ described here, the detailed chemical kinetic mechanism developed by the combustion group at Lawrence Livermore National Laboratory (LLNL) for homogeneous oxidation of i-octane (2,2,4-trimethylpentane)¹¹⁸ is applied; it consists of 7193 irreversible reactions among 857 species.

This study⁵³ also revealed that the applied chemical models – even though the most detailed ones available – need further improvement, in particular regarding the formation of minor by-products at rich conditions. Nevertheless, this combined modeling and experimental study elucidated the roles of surface, gas-phase, and radical chemistries in high-temperature oxidative catalytic conversion of iso-octane over Rh catalysts. From Fig. 12, it can clearly be concluded that the major products (syngas) are produced in the entrance region of the catalyst on the catalytic surface; radial concentration profiles are caused by a mass-transfer limited process. As soon as the oxygen is consumed on the catalytic surface – similar to CPOX of natural gas – hydrogen formation increases due to steam reforming; the major products are formed within few millimeters. At rich conditions ($C/O > 1.0$) a second process, now in the gas-phase, begins in the downstream part as shown in Fig. 13. The number of radicals in the gas-phase is sufficiently large to initiate gas-phase pyrolysis of the remaining fuel and formation of coke-precursors such as ethylene and propylene. In the experiment, the

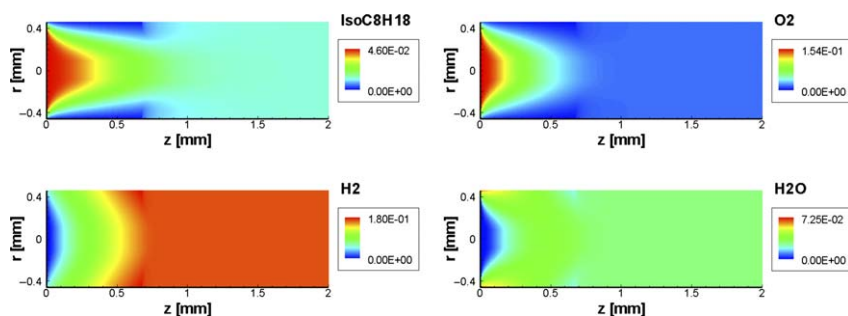


Fig. 12 Numerically predicted profiles of molar fractions of reactants and major products in the entrance region of the catalyst at $C/O = 1.2$ in CPOX of iso-octane over a Rh/alumina coated monolith, taken from Hartmann *et al.*⁵³ Flow direction is from left to right.

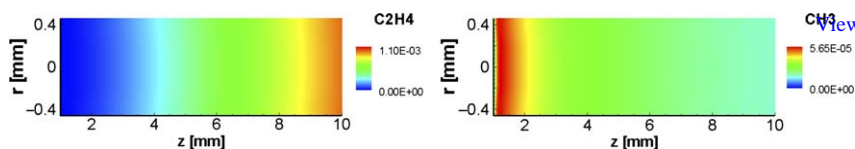


Fig. 13 Numerically predicted profiles of molar fractions of ethylene and the CH_3 -radical along the entire catalyst at $C/O=1.2$ in CPOX of iso-octane over a Rh/alumina coated monolith, taken from Hartmann *et al.*⁵³ Flow direction is from left to right.

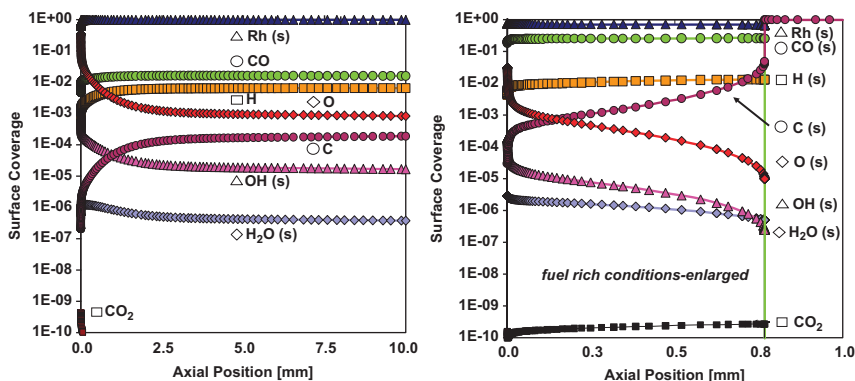


Fig. 14 Numerically predicted surface coverage as a function of axial position along the honeycomb catalyst channel in CPOX of iso-octane over a Rh/alumina coated monolith. Conditions: $C/O=0.8$, 1359 K (left), $C/O=1.2$, 1076 K (right); taken from reference 10.

downstream part of the catalyst is coked-up; here the Rh surface cannot act as sink for radicals. The study also numerically simulated the coverage of the Rh catalyst as function of the axial coordinate revealing a sufficient number of unoccupied surface sites at lean ($C/O=0.8$) conditions, Fig. 14 (left). At rich conditions ($C/O=1.2$, Fig. 14 (right)), however, the surface is fully covered by carbon further downstream.

4.3 Coking in high-temperature reforming over Rh catalysts

The model discussed above predicts a completely carbon, $\text{C}(s)$, covered surface in the downstream section of the catalyst, $z > 1$ mm. Since the model does not include interactions between gas-phase species and carbon on the surface directly, the gas-phase conversion practically proceeds independent of any direct influence of the catalytic surface, which means radicals are not recombined on the surface for $z > 1$ mm. However, both heterogeneous and homogeneous chemistries are coupled, because the resulting carbonaceous over-layer on the catalyst is a result of the composition of gas-phase near the channel wall. The exact position of this $\text{C}(s)$ layer is rather sensitive to small variations of several physical parameters such as reactor temperature, catalyst loading, flow rate, and diffusion models, and always occurs in the first third of the catalyst at given C/O ratio and is very typical for the rich regime as observed experimentally (Fig. 15).¹¹⁹ First studies indicate that the catalyst still shows some activity in that region. A recent AFM study¹²⁰

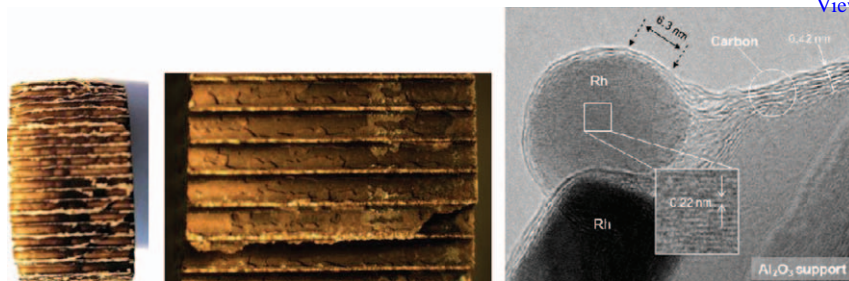


Fig. 15 Coke formation on the inner catalytic channel walls and TEM image of carbon covered Rh particle after the honeycomb was used in a CPOX reactor for several hours operated with iso-octane as feed at $C/O > 1.0$. Pictures are taken from Hartmann *et al.*¹¹⁹

of the initial state of coking in high-temperature reforming led to the conclusion that coke formation indeed starts at the catalyst particle and then spreads over the support. However, the mechanism of coke formation very much depends on the local conditions and temperature. Three different kinetic regimes have been recently observed in high-temperature reforming of hydrocarbons, two initiated by the catalytic particle, and one by deposition from the gas phase at higher temperatures and with a much larger rate.¹²¹

In particular, the olefins formed in the gas-phase at rich conditions have a high potential to form soot particles further downstream of the catalyst, because it will be difficult to cool-down the hot product fast enough to avoid any further gas-phase reactions and molecular growth of olefins to polycyclic aromatic hydrocarbons (PAH) will occur. The formed particulates definitely are a threat for any other devices such as fuel processing systems and fuel cells, which are located downstream of the CPOX reactor. Adequate measures have to be taken to either avoid operation of the CPOX reactor in a regime where gas-phase reactions are likely to produce precursors of particulate matter, to reduce olefin concentrations with post-catalyst conversion strategies, or to collect the particles formed, *e.g.* by the filters.

Gas-phase initiated coking of the product lines downstream of the catalytic section of the reactors caused by the olefin precursors formed in the catalytic section was the topic of a recent study by Kaltschmitt *et al.*¹²² The product composition of CPOX of iso-octane was chosen as the feed composition in a pure gas-phase experiment, in which the product stream was fed into an empty quartz tube heated up to a temperature typical for the catalyst exit temperature of the CPOX reactor to mimic the conditions downstream the catalyst. This homogeneous reactor was also modeled using two different large elementary-step reaction mechanisms. The study concluded that gas-phase reactions among a multitude of species are responsible for coke formation when unconverted fuel leaves the high temperature oxidation zone in the catalyst. Large amounts of olefinic hydrocarbons are initially formed by thermal cracking leading to aromatic molecules and further downstream to PAHs formation (Fig. 16). The presence of gas-phase reactions in the post-catalytic zone decreases the amount of hydrogen produced through methanation and hydrogenation of

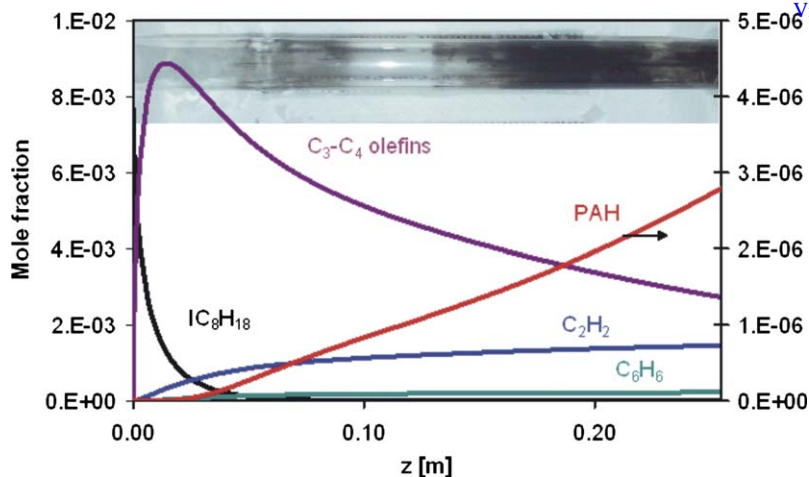


Fig. 16 Influence of gas-phase reactions on the catalyst exhaust composition in the post-catalyst zone of a CPOX reformer (Rh/alumina honeycomb) operated with iso-octane at rich conditions ($C/O = 1.6$). The catalyst exhaust composition measured was fed into an empty tube heated by a furnace to a temperature of 1106 K, which was the catalyst exit temperature measured in the CPOX reactor. The figure shows the numerically predicted distribution of carbon precursors along the empty tube clearly revealing post-catalyst conversion in the downstream gas-phase. C_3 - C_4 olefins contain 1,2-propadiene, propene, propyne, n-butene (1-buten, 2-butene), iso-butene, 1,3-butadiene; PAH contains naphthalene, anthracene, pyrene. Embedded photo shows the tubular quartz reactor after operation. Taken from Kaltschmitt *et al.*¹²²

carbon monoxide and olefins, especially at fuel rich conditions. Cracking of the remaining fuel increases the concentration of by-products (ethylene, acetylene and C_3 - C_4 olefins) and as a consequence of carbon deposits. A conclusion of their study is that the experimentally determined yields (major as well as minor products) in laboratory CPOX reactors may deviate from the local yields at the catalyst exit, because the products can usually not be quenched sufficiently fast to avoid gaseous post-reactions occurring within millimeters beyond the catalyst.

4.4 Impact of flow rate on reforming efficiency

In Fig. 8, the impact of flow rate on the temperature distribution in the monolithic sections of a short contact time reactor for reforming of iso-octane to hydrogen-rich synthesis gas reveals that higher flow rates lead to an increase in temperature, conversion and consequently higher hydrogen yields.¹⁰ This counter-intuitive increase in fuel conversion with decreasing residence time (increasing flow rate) can be explained by analyzing the ratio of chemical heat release to heat loss in the reactor.¹²³ Maier *et al.*¹⁰ showed that the right choice of the model to account for heat transfer in CPOX reactors helps to understand the impact of the flow rate on conversion and selectivity. An adiabatic single channel simulation will fail; it is not able to predict even the qualitative behavior, *i.e.*, the increase of the catalytic exit temperature with increasing flow rate as shown in Fig. 8.¹²³ Instead, the entire catalytic monolith with at least several representative channels has to be considered including heat transport within

the solid structure of the monolith and at all monolith boundaries. The increase in temperature with increasing flow rate can be understood by the effect of heat losses. The total amount of heat released by the reaction almost linearly increases with flow rate, because fuel is fully converted in the first zone of the catalyst. However, since higher temperature favors the less exothermic partial oxidation over the highly exothermic total oxidation, there is a kind of self-limiting process concerning the temperature increase. Consequently, the temperatures do not increase extraordinarily with increasing flow rate. The total amount of heat losses to the ambience by thermal conduction and radiation mainly depends on the temperature of the solid structure, which indeed is higher, but not so much higher to compensate for the larger heat release effect. In short, the ratio of chemical heat release to thermal heat loss increases with increasing flow rate, and therefore the temperature increases. Higher temperature in general leads to higher hydrogen yields due to thermodynamics. The product composition strongly depends on the flow rate, in particular at higher C/O ratios.¹²³ Also, the propensity of the formation of coke precursors is influenced by flow rate. As also shown in Fig. 8, the more exterior channels of the monolith exhibit lower temperatures, which consequently have an impact on the concentration profiles in the individual channels, not all channels behave essentially alike.

Higher temperatures do not only shift the thermodynamic equilibrium towards hydrogen production but also increase the reaction rate of the second global reaction step, *i.e.*, hydrogen production by steam reforming. The negative temperature gradient in the steam reforming zone is larger for higher flow rates even though the cooling effect by heat loss of the catalyst to the ambient is smaller for higher flow rates (Fig. 8). However, the heat loss effect clearly overlaps with the flow rate effect. At low flow rates, more exterior channels of the monolith experience much lower temperatures at slow than at high flow rates and, consequently, hydrogen production is reduced. In addition to steam reforming, also the exothermic water-gas-shift reaction leads to hydrogen production; this effect is rather small but still has a little impact on the final product composition and catalyst outlet temperature.¹²³ In summary, the understanding of the dependence of hydrogen selectivity on flow rate can only be achieved by taking mass and heat transfer as well as detailed kinetic schemes (reaction pathways) into account.

5 Reforming of diesel fuels

In comparison to natural gas and gasoline, diesel fuel has the higher hydrogen energy density. However, diesel is more difficult fuel to reform because diesel fuel is a mixture of a wide variety of paraffin, naphthene, and aromatics, each of which reacts differently in a CPOX reaction as discussed above and elsewhere.^{112,124,125} The usual occurrence of organosulfuric compounds will even more complicate the reforming, in particular concerning catalyst deactivation.

5.1 Reforming over Rh-based catalysts

Rhodium based catalysts were chosen for many studies of catalytic reforming of diesel and its major components, not only because it

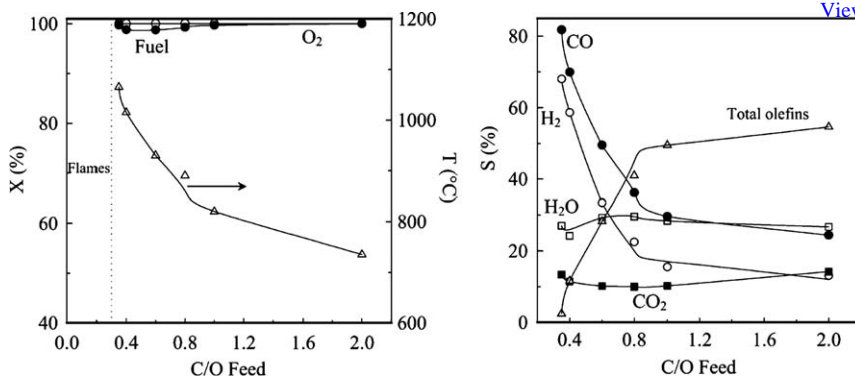


Fig. 17 Effect of the C/O ratio on the partial oxidation of diesel fuel over a Rh/alumina coated foam catalyst; conversion of fuel and oxygen and catalyst exit temperature measured (left) and product selectivity (right); taken from Krummenacher *et al.*¹

was successfully applied for reforming, in particular CPOX, of lighter hydrocarbons but also because it revealed low propensity of carbon formation.^{1,5,9,59,124,126,127}

The study of Krummenacher *et al.*¹ on CPOX of diesel over Rh/Al₂O₃ coated foam catalysts revealed that the highest hydrogen yields can be achieved when the reactor is operated at low C/O ratios, which are actually close to the flammability of the mixture as shown in Fig. 17. The maximum in syngas yield occurs at the transition to the occurrence of flames. Furthermore, the operation of diesel fuel at such low C/O ratios presents a challenge for the mixing and feeding of the reactants, in particular, a much higher tendency to pre-combustion of the fuel upstream the catalytic section is observed. This transient behaviour is less drastic when the single fuel components or binary mixtures of those are used. The hydrogen yields show a maximum at C/O ratios closer to 1.0 and the reactor can be operated more safely.^{1,59,112}

CPOX of diesel also is more affected by the formation of carbonaceous overlayers and coking of the reactor lines downstream the catalyst. Indeed, incomplete conversion of the fuel in the catalytic section will eventually lead to coke formation unless secondary measures are applied. Since oxygen consumption is usually complete, the C/O ratio moves to infinity along the reactor. The pyrolytic conditions will eventually lead to the production of the coke precursors ethylene and propylene as shown in Fig. 17 and discussed above. Even when the production of the olefins is on a ppm-level, the accumulative effect may lead to coking issues after a certain time of operation of a technical system.

Aside from pure CPOX operation, the addition of steam and/or exhaust of, for instance, a downstream operated fuel cell stack, may be beneficial not only for efficiency due to improved heat balances but also for prevention of coking. However, one has to take into account that the oxygen in H₂O and CO₂ may reveal a different reactivity than the oxygen of molecular O₂.

With steam addition, operation of the reformer moves towards ATR and even the SR regime. Thormann *et al.*^{5,127,128} studied steam reforming of diesel and hexadecane over a Rh/CeO₂ catalyst in a microchannel reactor

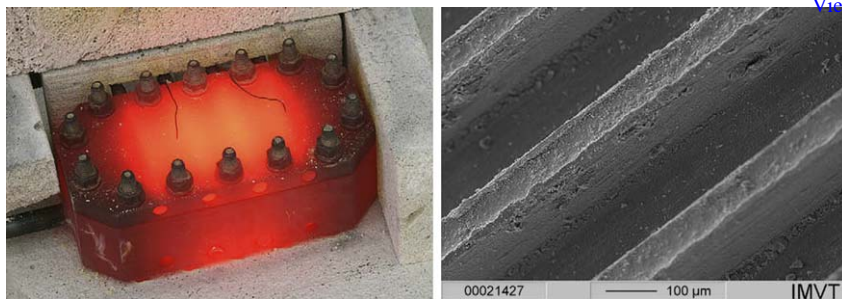


Fig. 18 Picture of a microreactor applied for steam reforming of diesel at operation temperature of 973 K (left) and SEM micrograph of the catalytically active reactor channels coated with Rh/CeO₂ (right). Taken from Thormann *et al.*⁵

shown in Fig. 18. In a combined experimental and modeling study⁵ a significant impact of the ceria support on the reformat composition was observed.

5.2 Alternate catalysts

Due to the cost of Rh a variety of alternate catalytic materials have been investigated recently such as hexaaluminates^{129,130} and pyrochlores.¹⁸ These oxides are of particular interest because the catalytically active metals can be substituted within the structure of these materials to produce a thermally stable catalyst that resists both sulfur poisoning and carbon deposition.¹²⁶

6 Reforming of ethanol and ethanol blended gasoline

Ethanol has been directly used as fuel and as fuel component for many years. Today, there is a further increasing interest in ethanol containing fuel due to its potential of the reduction of greenhouse gases, because it can be easily obtained in large amounts by fermentation of biomass. The decisive difference in ethanol as feed for reformers in comparison with the fuels discussed so far, is the fact that ethanol contains an oxygen atom, which may lead to quite a different product composition.

Quite a variety of studies on reforming ethanol towards hydrogen and synthesis gas were conducted using steam reforming,^{131–138} partial oxidation^{139–143} and autothermal reforming.^{144–150} Another difference of ethanol reforming is the fact, that in contrast to POX of aliphatic hydrocarbons such as methane (natural gas), iso-octane (gasoline), and hexadecane (diesel), the partial oxidation of ethanol is slightly endothermic.

In the remainder of this section, we will present some recent results of CPOX of ethanol and ethanol-blended fuels obtained in our group.^{151,152}

6.1 CPOX of ethanol over Rh/Al₂O₃ coated monoliths

Hebben *et al.*¹⁵¹ used the same apparatus as described above (Section 4.1) in their study on CPOX of ethanol on alumina-supported rhodium based catalyst. They showed that the selectivity to hydrogen is almost as high as in the thermodynamic equilibrium without by-product formation for C/O < 0.8. At higher C/O > 0.8, the conversion of ethanol drops while the

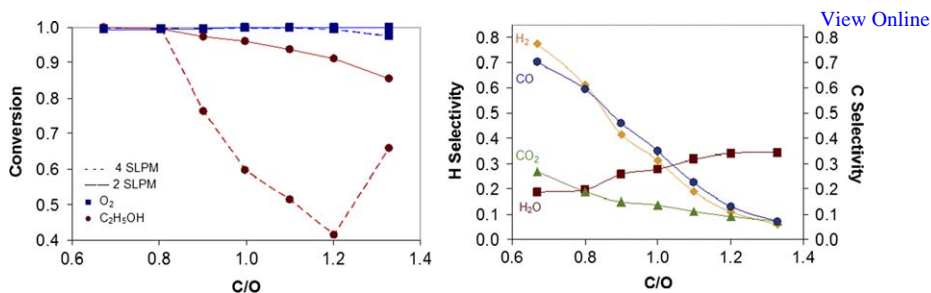


Fig. 19 Experimentally measured fuel conversion (left) and selectivity of major products as function of C/O for the CPOX of ethanol on alumina-supported Rh based honeycomb catalysts for two different flow rates (left) and at 2 slpm (right); taken from Hebben *et al.*¹⁵¹

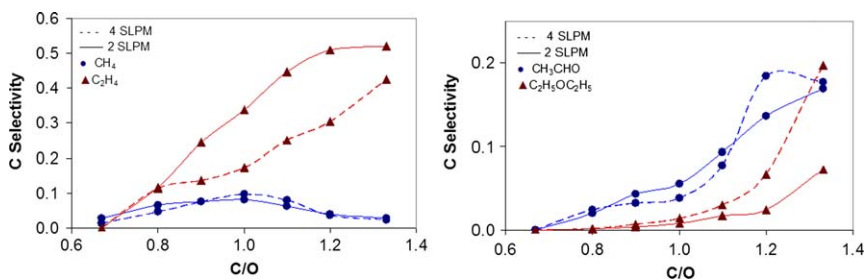


Fig. 20 Experimentally measured selectivity of by-products as function of C/O for the CPOX of ethanol on alumina-supported Rh coated honeycomb catalysts for two different flow rates; taken from Hebben *et al.*¹⁵¹

oxygen conversion is complete at all C/O ratios studied (Fig. 19), and the by-products are significantly produced as shown in Fig. 20. Aside from the already reported production of methane, ethylene, and acetaldehyde at increasing C/O, significant amounts of diethyl ether have been detected in CPOX of ethanol at C/O > 1.20.

The time to reach steady state depends on the C/O. At C/O > 1.0, slow deactivation of the catalyst occurs due to coke formation, *i.e.*, a steady state in conversion and selectivity is not reached at all and product composition and fuel conversion slowly vary in time. Regeneration of the catalyst is needed after a certain time. Gas-phase reactions play basically no role for fuel conversion at sufficiently high flow rates for ethanol reforming at the given conditions.¹⁵¹

The alumina support seems to have a significant influence for the CPOX of ethanol on alumina-supported rhodium based catalysts, in case of high C/O and fuel-dilution.¹⁵¹

6.2 CPOX of ethanol blended gasoline over Rh/Al₂O₃ coated monoliths

The characteristic features of ethanol reforming leads to the question of their impact on reforming of gasoline that is blended with ethanol. The increasing use of renewable fuels, *e.g.* ethanol, and fossil fuels blended with renewable fuels, *e.g.* E 10 (gasoline blended with 10 vol.-% ethanol), in

vehicles also intensifies the research activities for these fuels in the field of on-board hydrogen supply.^{145,151,153–161}

In a recent study, Diehm *et al.*¹⁵² systematically studied the impact of ethanol content in gasoline on CPOX of gasoline over a Rh/alumina coated monolith. The experimental equipment as described above for the iso-octane study was used. In the research work presented in this paper, the performance of ethanol blended gasoline is studied in a CPOX reformer. Real gasoline fuel as well as iso-octane as gasoline surrogate was used and mixed with ethanol. Ethanol in iso-octane blends with ethanol concentrations varying from 5 to 85 vol. % were studied for several operating conditions ranging from fuel lean to fuel rich conditions. In addition, analogue investigations of the pure substances ethanol and iso-octane were performed. Additionally, the commercial fuels, “Super” gasoline (gasoline blended with 5 vol. % ethanol) and E 85 (gasoline blended with 85 vol. % ethanol), were examined as well.

Ethanol is faster converted than iso-octane (Fig. 21), in particular the conversion of iso-octane drops already at relatively low C/O ratios, and increasing ethanol content increases this effect. The hydrogen selectivity generally decreases with increasing ethanol content, however, this trend is not linear. Actually, the highest hydrogen yield is achieved at 5% ethanol and not at pure iso-octane (Fig. 22). The formation of by-products is also promoted by ethanol, rather high ethylene concentrations are found even at low C/O ratios. All these findings were also observed using ethanol blended commercial gasoline (E5, E10, E85).¹⁵²

The conclusions to be drawn by this study are: (1) Ethanol-blended iso-octane can serve as surrogate for ethanol blended gasoline. (2) Ethanol has a severe impact on conversion and selectivity of reforming of logistic fuels. (3) This impact cannot be estimated by the reforming performance of the pure substances; simple linear interpolation from the behavior of the pure substances to the behavior of the mixtures does not work.

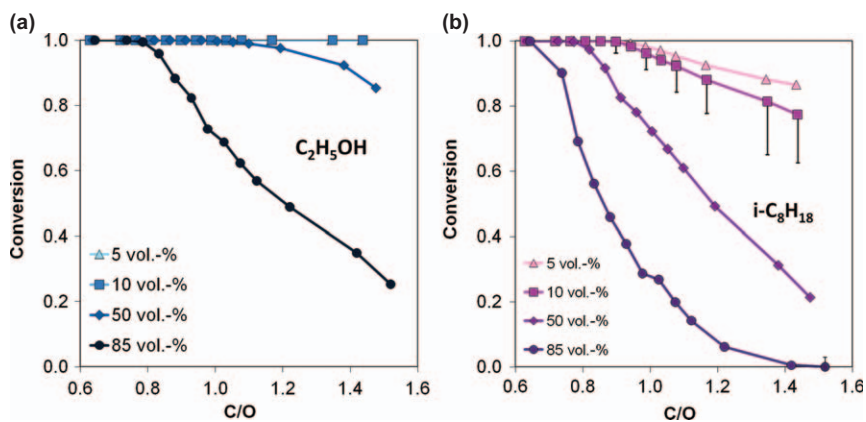


Fig. 21 C-based conversion of ethanol (a) and iso-octane (b) as function of C/O ratio for CPOX of ethanol/iso-octane blends over Rh/Al₂O₃ coated honeycomb monolith. Vol.-% nomenclature denotes the molar percentage of ethanol in the blend. Taken from Diehm *et al.*¹⁵²

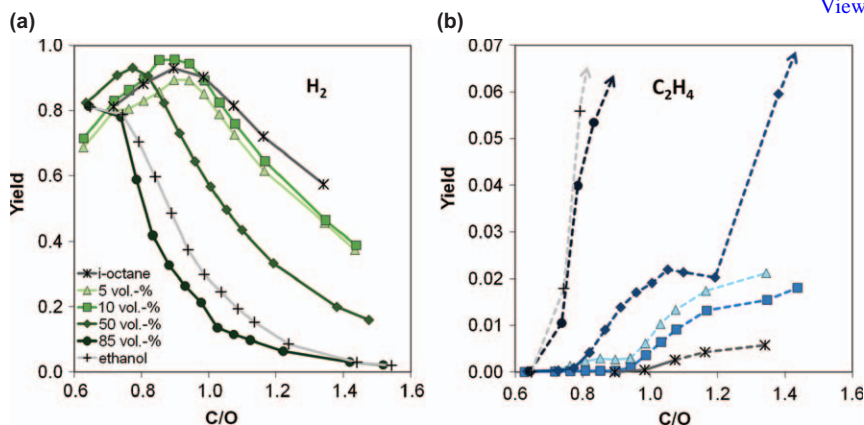


Fig. 22 C-based yields of hydrogen (a) and ethylene (b) for ethanol/iso-octane blends and pure substances as function of C/O ratio in a CPOX reactor with a Rh/Al₂O₃ coated honeycomb monolith. The dotted lines represent qualitative values. The arrows indicate the trend of further rising yields. Vol.-% nomenclature (a) denotes the molar percentage of ethanol in the blend; symbols also apply for nomenclature of Fig. (b). Taken from Diehm *et al.*¹⁵²

7 Summary

High-temperature catalysis is a promising technique for high-throughput reforming of logistic fuels (natural gas, gasoline, diesel, kerosene, ethanol) in compact devices without the need of external energy. Aside from producing hydrogen-rich synthesis gas, high-temperature catalysis can also be applied for the production of more useful basic chemicals such as olefins and acetylene from logistic fuels such as natural gas. Partial oxidation of these fuels at millisecond contact times over Rh-based catalysts at around 1000 °C and at optimal fuel/oxygen ratios leads to almost total fuel conversion and hydrogen yields being close to the ones at thermodynamic equilibrium.

Conversion and selectivity strongly depend on the molar C/O ratio of the fuel/oxygen (air) mixture. In general, the optimal C/O ratio for hydrogen yield is around the stoichiometric ratio of unity, the production of total oxidation products (H₂O, CO₂) and un-desired hydrocarbons (soot precursors such as olefins) are favored at lean (C/O < 1) and rich (C/O > 1) conditions, respectively. However, depending on the type of fuel, the optimal C/O ratio for achieving the maximum hydrogen yield at a minimum amount of undesired by-products (olefins, acetylene, aromatics) can relatively strong deviate from this optimal C/O ratio. Also, the actual composition of a commercial fuel strongly influences hydrogen yield and product selectivity. Here, the structure of the individual fuel components matter more than their chain length. Therefore, the behavior of real fuels in CPOX reformers is difficult to derive from the behavior of single component surrogates. In particular, diesel and ethanol-blended fuels exhibit a complex behavior, which cannot linearly extrapolated from the behavior of their single components. In reforming of ethanol, significant amounts of ethylene and acetaldehyde are produced even at low C/O ratios.

The deactivation of the catalyst and of downstream pipes and devices (*e.g.* fuel cells) due to coking is one of the challenges in the technical

realization of CPOX-based APUs. The coking is initiated by the formation of olefins in the gas-phase due to oxidative and –even more important– pyrolytic processes; exceptions are methane (no coking at relevant pressure) and ethanol (surface processes seem to matter as well).

Modeling and simulation can support the understanding of the interaction of mass and heat transfer with heterogeneous and homogeneous chemical reactions in the reformer. The dependence of product composition on C/O ratio, temperature, and flow rate as well as the occurrence of coke precursors can be explained by modeling work, at least qualitatively. The catalytic conversion is usually controlled by mass-transfer (external diffusion). Most reformers operated with fuels that contain aliphatic and aromatic hydrocarbons with two and more carbon atoms exhibit a coupling between catalytic and homogeneous (gas-phase) conversion via adsorbed and desorbed intermediates and radicals. Detailed catalytic reaction mechanisms over rhodium-based catalysts are only available for natural gas and single-component liquid fuel surrogates such as iso-octane. The extrapolation of the behavior of reformers operated with surrogates (laboratory scale) to the behavior of reformers operated with complex logistic fuels has to be conducted with care. However, studies using surrogates can indeed lead to useful information for the design of reformers and the optimization of operational conditions to maximize hydrogen yield and minimize by-product formation as discussed in this chapter.

Acknowledgement

The work presented includes studies of former and current PhD students and postdocs in my group at the Karlsruhe Institute of Technology; in particular I would like to express my appreciation to L. Maier, S. Tischer, R. Schwiedernoch, B. Schädel, M. Hartmann, T. Kaltschmitt, N. Hebben, C. Diehm, and C. Eßmann and thanks to Y. Dedecek for editorial assistance. I very much appreciate many fruitful discussions on high-temperature catalysis with L.D. Schmidt (University of Minnesota), R.J. Kee and A.M. Dean (Colorado School of Mines), J. Mantzaras (PSI Switzerland), R. Horn (FHI Berlin), and A. Beretta (Politecnico Milano). Financial support by the German Research Foundation (DFG) and many industrial partners is gratefully acknowledged.

References

- 1 J. J. Krummenacher, K. N. West and L. D. Schmidt, *J. Catal.*, 2003, **215**, 332–343.
- 2 A. Lindermeir, S. Kah, S. Kavurucu and M. Muhlner, *Appl. Catal. B-Environ.*, 2007, **70**, 488–497.
- 3 A. D. Qi, S. D. Wang, C. J. Ni and D. Y. Wu, *Int. J. Hydrog. Energy*, 2007, **32**, 981–991.
- 4 B. J. Dreyer, I. C. Lee, J. J. Krummenacher and L. D. Schmidt, *Appl. Catal. A-Gen.*, 2006, **307**, 184–194.
- 5 J. Thormann, L. Maier, P. Pfeifer, U. Kunz, O. Deutschmann and K. Schubert, *Int. J. Hydrog. Energy*, 2009, **34**, 5108–5120.
- 6 L. Bobrova, I. Zolotarisky, V. Sadykov and V. Sobyenin, *Int. J. Hydrog. Energy*, 2007, **32**, 3698–3704.

- 7 S. Jain, H. Y. Chen and J. Schwank, *J. Power Sources*, 2006, **160**, 474–484. [View Online](#)
- 8 L. F. Brown, *Int. J. Hydrog. Energy*, 2001, **26**, 381–397.
- 9 R. P. O'Connor, E. J. Klein and L. D. Schmidt, *Catal. Lett.*, 2000, **70**, 99–107.
- 10 L. Maier, M. Hartmann, S. Tischer and O. Deutschmann, *Combust. Flame*, 2011, **158**, 796–808.
- 11 C. Severin, S. Pischinger and J. Ogrzewalla, *J. Power Sources*, 2005, **145**, 675–682.
- 12 Delphi Automotive LLP, <http://delphi.com/manufacturers/cv/fuelcells/>, 06.10.2011.
- 13 D. A. Hickman and L. D. Schmidt, *J. Catal.*, 1992, **138**, 267–282.
- 14 O. Deutschmann and L. D. Schmidt, *American Institute of Chemical Engineering Journal*, 1998, **44**, 2465–2477.
- 15 M. C. Huff and L. D. Schmidt, *J. Catal.*, 1993, **149**, 127–141.
- 16 D. K. Zerkle, M. D. Allendorf, M. Wolf and O. Deutschmann, *J. Catal.*, 2000, **196**, 18–39.
- 17 R. M. N. Yerga, M. C. Alvarez-Galvan, N. Mota, J. A. V. de la Mano, S. M. Al-Zahrani and J. L. G. Fierro, *Chemcatchem*, 2010, **3**, 440–457.
- 18 D. J. Haynes, D. A. Berry, D. Shekhawat and J. J. Spivey, *Catal. Today*, 2009, **145**, 121–126.
- 19 D. J. Haynes, A. Campos, M. W. Smith, D. A. Berry, D. Shekhawat and J. J. Spivey, *Catal. Today*, 2010, **154**, 210–216.
- 20 J. Windmann, J. Braun, P. Zacke, S. Tischer, O. Deutschmann and J. Warnatz, *SAE Technical Paper*, 2003, 2003–01–0937.
- 21 R. B. Bird, W. E. Stewart and E. N. Lightfoot, *Transport Phenomena*, John Wiley & Sons, Inc., New York, 2001.
- 22 S. V. Patankar, *Numerical Heat Transfer and Fluid Flow*, McGraw-Hill, New York, 1980.
- 23 J. Warnatz, R. W. Dibble and U. Maas, *Combustion, Physical and Chemical Fundamentals, Modeling and Simulation, Experiments, Pollutant Formation*, Springer-Verlag, New York, 1996.
- 24 R. E. Hayes and S. T. Kolaczowski, *Introduction to Catalytic Combustion*, Gordon and Breach Science Publ., Amsterdam, 1997.
- 25 R. J. Kee, M. E. Coltrin and P. Glarborg, *Chemically Reacting Flow*, Wiley-Interscience, 2003.
- 26 O. Deutschmann, in *Handbook of Heterogeneous Catalysis*, ed. H. K. G. Ertl, F. Schüth, J. Weitkamp, Wiley-VCH, Weinheim, 2008, pp. 1811–1828.
- 27 O. Deutschmann, ed., *Modeling and Simulation of Heterogeneous Catalytic Reactions: From the molecular process to the technical system*, Wiley-VCH, Weinheim, 2011.
- 28 E. Ranzi, A. Sogaro, P. Gaffuri, G. Pennati, C. K. Westbrook and W. J. Pitz, *Combust. Flame*, 1994, **99**, 201–211.
- 29 M. E. Coltrin, R. J. Kee and F. M. Rupley, *SURFACE CHEMKIN (Version 4.0): A Fortran Package for Analyzing Heterogeneous Chemical Kinetics at a Solid-Surface - Gas-Phase Interface*, SAND91-8003B, Sandia National Laboratories, 1991.
- 30 A. B. Mhadeshwar, H. Wang and D. G. Vlachos, *Journal of Physical Chemistry B*, 2003, **107**, 12721–12733.
- 31 L. Maier, B. Schädel, K. Herrera Delgado, S. Tischer and O. Deutschmann, *Topics in Catalysis*, 2011, **54**, 845–858.
- 32 W. R. Williams, C. M. Marks and L. D. Schmidt, *J. Phys. Chem.*, 1992, **96**, 5922–5931.
- 33 B. Hellsing, B. Kasemo and V. P. Zhdanov, *J. Catal.*, 1991, **132**, 210–228.
- 34 J. Warnatz, *Proc. Combust. Inst.*, 1992, **24**, 553–579.

- 35 M. Rinnemo, O. Deutschmann, F. Behrendt and B. Kasemo, *Combust. Flame*, 1997, **111**, 312–326.
- 36 G. Vesper, *Chem. Eng. Sci.*, 2001, **56**, 1265–1273.
- 37 P.-A. Bui, D. G. Vlachos and P. R. Westmoreland, *Industrial & Engineering Chemistry Research*, 1997, **36**, 2558–2567.
- 38 J. C. G. Andrae and P. H. Björnbohm, *American Institute of Chemical Engineering Journal*, 2000, **46**, 1454–1460.
- 39 J. Mai, W. von Niessen and A. Blumen, *J. Chem. Phys.*, 1990, **93**, 3685–3692.
- 40 V. P. Zhdanov and B. Kasemo, *Applied Surface Science*, 1994, **74**, 147–164.
- 41 P. Aghalayam, Y. K. Park and D. G. Vlachos, *Proc. Combust. Inst.*, 2000, **28**, 1331–1339.
- 42 O. Deutschmann, R. Schmidt, F. Behrendt and J. Warnatz, *Proceedings of the Combustion Institute*, 1996, **26**, 1747–1754.
- 43 G. Vesper, J. Frauhammer, L. D. Schmidt and G. Eigenberger, in *Studies in Surface Science and Catalysis 109*, 1997, pp. 273–284.
- 44 P.-A. Bui, D. G. Vlachos and P. R. Westmoreland, *Surface Science*, 1997, **386**, L1029–L1034.
- 45 U. Dogwiler, P. Benz and J. Mantzaras, *Combustion and Flame*, 1999, **116**, 243.
- 46 P. Aghalayam, Y. K. Park, N. Fernandes, V. Papavassiliou, A. B. Mhadeshwar and D. G. Vlachos, *J. Catal.*, 2003, **213**, 23–38.
- 47 D. A. Hickman and L. D. Schmidt, *American Institute of Chemical Engineering Journal*, 1993, **39**, 1164–1176.
- 48 M. Huff and L. D. Schmidt, *J. Phys. Chem.*, 1993, **97**, 11815–11822.
- 49 M. C. Huff, I. P. Androulakis, J. H. Sinfelt and S. C. Reyes, *J. Catal.*, 2000, **191**, 46–54.
- 50 F. Donsi, K. A. Williams and L. D. Schmidt, *Ind. Eng. Chem. Res.*, 2005, **44**, 3453–3470.
- 51 R. Schwiedernoch, S. Tischer, C. Correa and O. Deutschmann, *Chem. Eng. Sci.*, 2003, **58**, 633–642.
- 52 E. S. Hecht, G. K. Gupta, H. Y. Zhu, A. M. Dean, R. J. Kee, L. Maier and O. Deutschmann, *Appl. Catal. A-Gen.*, 2005, **295**, 40–51.
- 53 M. Hartmann, L. Maier, H. D. Minh and O. Deutschmann, *Combust. Flame*, 2010, **157**, 1771–1782.
- 54 A. Donazzi, D. Livio, M. Maestri, A. Beretta, G. Groppi, E. Tronconi and P. Forzatti, *Angewandte Chemie-International Edition*, 2011, **50**, 3943–3946.
- 55 A. Beretta, P. Forzatti and E. Ranzi, *J. Catal.*, 1999, **184**, 469–478.
- 56 A. Beretta and P. Forzatti, *J. Catal.*, 2001, **200**, 45–58.
- 57 A. Beretta, E. Ranzi and P. Forzatti, *Chem. Eng. Sci.*, 2001, **56**, 779–787.
- 58 R. Subramanian and L. D. Schmidt, *Angewandte Chemie-International Edition*, 2005, **44**, 302–305.
- 59 J. J. Krummenacher and L. D. Schmidt, *J. Catal.*, 2004, **222**, 429–438.
- 60 L. D. Schmidt, J. Siddall and M. Bearden, *American Institute of Chemical Engineering Journal*, 2000, **46**, 1492–1495.
- 61 D. Papadias, L. Edsberg and P. H. Björnbohm, *Catal. Today*, 2000, **60**, 11–20.
- 62 F. Keil, *Diffusion und Chemische Reaktionen in der Gas-Feststoff-Katalyse*, Springer-Verlag, Berlin, 1999.
- 63 F. J. Keil, *Catal. Today*, 2000, **53**, 245–258.
- 64 N. Mladenov, J. Koop, S. Tischer and O. Deutschmann, *Chem. Eng. Sci.*, 2010, **65**, 812–826.
- 65 O. Deutschmann, R. Schwiedernoch, L. I. Maier and D. Chatterjee, *Studies in Surface Science and Catalysis*, 2001, **136**, 251–258.

- 66 O. Deutschmann, S. Tischer, S. Kleditzsch, V. M. Janardhanan, C. Correa, D. Chatterjee, N. Mladenov and H. D. Minh, DETCHEM™ software package, www.detchem.com, 2008.
- 67 U. Maas and S. Pope, *Combust. Flame*, 1992, **88**, 239–264.
- 68 X. Yan and U. Maas, *Proc. Combust. Inst.*, 2000, **28**, 1615–1621.
- 69 R. G. Susnow, A. M. Dean, W. H. Green, P. Peczak and L. Broadbelt, *J. Phys. Chem. A*, 1997, **101**, 3731–3740.
- 70 S. Tischer, C. Correa and O. Deutschmann, *Catal. Today*, 2001, **69**, 57–62.
- 71 S. Tischer and O. Deutschmann, *Catal. Today*, 2005, **105**, 407–413.
- 72 C. Appel, J. Mantzaras, R. Schaeren, R. Bombach, B. Kaeppli and A. Inauen, *Proc. Combust. Inst.*, 2002, **29**, 1031–1038.
- 73 C. Appel, J. Mantzaras, R. Schaeren, R. Bombach, A. Inauen, B. Kaeppli, B. Hemmerling and A. Stampanoni, *Combust. Flame*, 2002, **128**, 340–368.
- 74 A. Schneider, J. Mantzaras and S. Eriksson, *Combustion Science and Technology*, 2008, **180**, 89–126.
- 75 A. Schneider, J. Mantzaras, R. Bombach, S. Schenker, N. Tylli and P. Jansohn, *Proc. Combust. Inst.*, 2007, **31**, 1973–1981.
- 76 S. Eriksson, A. Schneider, J. Mantzaras, M. Wolf and S. Jaras, *Chem. Eng. Sci.*, 2007, **62**, 3991–4011.
- 77 C. Appel, J. Mantzaras, R. Schaeren, R. Bombach, A. Inauen, N. Tylli, M. Wolf, T. Griffin, D. Winkler and R. Carroni, *Proc. Combust. Inst.*, 2005, **30**, 2509–2517.
- 78 M. Reinke, J. Mantzaras, R. Schaeren, R. Bombach, A. Inauen and S. Schenker, *Combust. Flame*, 2004, **136**, 217–240.
- 79 A. Schneider, J. Mantzaras and P. Jansohn, *Chem. Eng. Sci.*, 2006, **61**, 4634–4649.
- 80 R. Horn, O. Korup, M. Geske, U. Zavyalova, I. Oprea and R. Schlogl, *Rev. Sci. Instrum.*, 2010, **81**, 6.
- 81 H. D. Minh, H. G. Bock, S. Tischer and O. Deutschmann, *Aiche J.*, 2008, **54**, 2432–2440.
- 82 H. D. Minh, H. G. Bock, S. Tischer and O. Deutschmann, *Computational Science and Its Applications - Iccsa 2008, Pt 1, Proceedings*, 2008, **5072**, 1121–1130.
- 83 M. von Schwerin, O. Deutschmann and V. Schulz, *Comput. Chem. Eng.*, 2000, **24**, 89–97.
- 84 J. R. Rostrup-Nielsen, ed., *Catalytic Steam Reforming*, Springer-Verlag, New York, 1984.
- 85 D. L. Trimm, *Catal. Today*, 1997, **37**, 233–238.
- 86 E. Ochoa-Fernandez, H. K. Rusten, H. A. Jakobsen, M. Ronning, A. Holmen and D. Chen, *Catal. Today*, 2005, **106**, 41–46.
- 87 D. Dissanayake, K. C. C. Kharas, J. H. Lunsford and M. P. Rosynek, *J. Catal.*, 1993, **139**, 652–663.
- 88 D. A. Hickman and L. D. Schmidt, *Science*, 1993, **259**, 343–346.
- 89 D. A. Hickman and L. D. Schmidt, *J. Catal.*, 1992, **138**, 267–282.
- 90 O. Deutschmann and L. D. Schmidt, *Aiche J.*, 1998, **44**, 2465–2477.
- 91 S. Hannemann, J. D. Grunwaldt, N. van Vegten, A. Baiker, P. Boye and C. G. Schroer, *Catal. Today*, 2007, **126**, 54–63.
- 92 R. Horn, K. A. Williams, N. J. Degenstein and L. D. Schmidt, *J. Catal.*, 2006, **242**, 92–102.
- 93 D. A. Hickman and L. D. Schmidt, *Aiche J.*, 1993, **39**, 1164–1177.
- 94 A. B. Mhadeshwar and D. G. Vlachos, *Ind. Eng. Chem. Res.*, 2007, **46**, 5310–5324.
- 95 A. B. Mhadeshwar and D. G. Vlachos, *Journal of Physical Chemistry B*, 2005, **109**, 16819–16835.

- 96 M. Maestri, D. G. Vlachos, A. Beretta, G. Groppi and E. Tronconi, *J. Catal.*, 2008, **259**, 211–222.
- 97 O. Deutschmann, F. Behrendt and J. Warnatz, *Catal. Today*, 1994, **21**, 461–470.
- 98 R. Quiceno, J. Perez-Ramirez, J. Warnatz and O. Deutschmann, *Appl. Catal. A-Gen.*, 2006, **303**, 166–176.
- 99 N. E. McGuire, N. P. Sullivan, O. Deutschmann, H. Y. Zhu and R. J. Kee, *Appl. Catal. A-Gen.*, 2011, **394**, 257–265.
- 100 J. G. Xu and G. F. Froment, *Aiche J.*, 1989, **35**, 97–103.
- 101 J. G. Xu and G. F. Froment, *Aiche J.*, 1989, **35**, 88–96.
- 102 J. R. Rostrup-Nielsen and J.-H. B. Hansen, *J. Catal.*, 1993, **144**, 38–49.
- 103 D. Mogensen, J. D. Grunwaldt, P. V. Hendriksen, K. Dam-Johansen and J. U. Nielsen, *J. Power Sources*, 2011, **196**, 25–38.
- 104 J. M. Wei and E. Iglesia, *J. Catal.*, 2004, **224**, 370–383.
- 105 B. C. Enger, R. Lodeng and A. Holmen, *Appl. Catal. A-Gen.*, 2008, **346**, 1–27.
- 106 D. Chen, R. Lodeng, H. Svendsen and A. Holmen, *Ind. Eng. Chem. Res.*, 2011, **50**, 2600–2612.
- 107 V. M. Janardhanan and O. Deutschmann, *J. Power Sources*, 2006, **162**, 1192–1202.
- 108 L. D. Schmidt, O. Deutschmann and C. T. Goralski, in *Natural Gas Conversion V*, 1998, pp. 685–692.
- 109 B. T. Schadel, M. Duisberg and O. Deutschmann, *Catal. Today*, 2009, **142**, 42–51.
- 110 B. T. Schadel and O. Deutschmann, in *Natural Gas Conversion Viii, Proceedings of the 8th Natural Gas Conversion Symposium*, eds. F. B. Noronha, M. Schmal and E. F. SousaAguar, 2007, pp. 207–212.
- 111 G. Goldin, H. Zhu, K. Katte, A. Dean, R. Braun, R. Kee, D. Zhang, L. Maier and O. Deutschmann, *ECS Transactions*, 2009, **25**, 1253–1262.
- 112 M. Hartmann, T. Kaltschmitt and O. Deutschmann, *Catal. Today*, 2009, **147**, S204–S209.
- 113 M. Hartmann, S. Lichtenberg, N. Hebben, D. Zhang and O. Deutschmann, *Chem. Ing. Tech.*, 2009, **81**, 909–919.
- 114 S. M. Villano, J. Hoffmann, H. H. Carstensen and A. M. Dean, *J. Phys. Chem. A*, 2010, **114**, 6502–6514.
- 115 I. Y. Kang, H. H. Carstensen and A. M. Dean, *J. Power Sources*, 2011, **196**, 2020–2026.
- 116 I. Kang, H. H. Carstensen and A. M. Dean, *Thermec 2009, Pts 1-4*, **638–642**, 1118–1124.
- 117 L. L. Raja, R. J. Kee, O. Deutschmann, J. Warnatz and L. D. Schmidt, *Catal. Today*, 2000, **59**, 47–60.
- 118 H. J. Curran, P. Gaffuri, W. J. Pitz and C. K. Westbrook, *Combust. Flame*, 2002, **129**, 253–280.
- 119 M. Hartmann, in *Erzeugung von Wasserstoff mittels katalytischer Partialoxidation höherer Kohlenwasserstoffe an Rhodium. Doctoral thesis. Fakultät für Chemie und Biowissenschaften, Universität Karlsruhe (TH)*, 2009.
- 120 C. Essmann, in *Untersuchung der Verkokung von Rhodiumkatalysatoren während der Wasserdampfreformierung von Erdgas. Doctoral thesis. Fakultät für Chemie und Biowissenschaften, Karlsruhe Institute of Technology*, 2011.
- 121 B. Schädel, in *Wasserdampfreformierung von Erdgas mit Rhodiumkatalysatoren: Aktivität und Deaktivierung. Doctoral thesis. Department of Chemistry and Biosciences. University of Karlsruhe, University of Karlsruhe, Karlsruhe*, 2008.
- 122 T. Kaltschmitt, L. Maier, M. Hartmann, C. Hauck and O. Deutschmann, *Proc. Combust. Inst.*, 2010, **33**, 3177–3183.

- 123 M. Hartmann, L. Maier and O. Deutschmann, *Appl. Catalysis A: General*, 2011, **391**, 144–152.
- 124 R. Subramanian, G. J. Panuccio, J. J. Krummenacher, I. C. Lee and L. D. Schmidt, *Chem. Eng. Sci.*, 2004, **59**, 5501–5507.
- 125 D. Shekhawat, D. A. Berry, D. J. Haynes and J. J. Spivey, *Fuel*, 2009, **88**, 817–825.
- 126 D. Shekhawat, T. H. Gardner, D. A. Berry, M. Salazar, D. J. Haynes and J. J. Spivey, *Appl. Catal. A-Gen.*, 2006, **311**, 8–16.
- 127 J. Thormann, P. Pfeifer, K. Schubert and U. Kunz, *Chemical Engineering Journal*, 2008, **135**, S74–S81.
- 128 J. Thormann, P. Pfeifer, U. Kunz and K. Schubert, *International Journal of Chemical Reactor Engineering*, 2008, **6**.
- 129 R. W. Sidwell, H. Y. Zhu, B. A. Kibler, R. J. Kee and D. T. Wickham, *Appl. Catal. A-Gen.*, 2003, **255**, 279–288.
- 130 T. H. Gardner, J. J. Spivey, A. Campos, J. C. Hissam, E. L. Kugler and A. D. Roy, *Catal. Today*, 2010, **157**, 166–169.
- 131 S. Cavallaro, *Energy & Fuels*, 2000, **14**, 1195–1199.
- 132 D. K. Liguras, D. I. Kondarides and X. E. Verykios, *Appl. Catal. B-Environ.*, 2003, **43**, 345–354.
- 133 S. Cavallaro, V. Chiodo, S. Freni, N. Mondello and F. Frusteri, *Appl. Catal. A-Gen.*, 2003, **249**, 119–128.
- 134 E. C. Wanat, K. Venkataraman and L. D. Schmidt, *Appl. Catal. A-Gen.*, 2004, **276**, 155–162.
- 135 N. Laosiripojana and S. Assabumrungrat, *Appl. Catal. B-Environ.*, 2006, **66**, 29–39.
- 136 A. Birot, F. Epron, C. Descorme and D. Duprez, *Appl. Catal. B-Environ.*, 2008, **79**, 17–25.
- 137 S. Liu, K. Zhang, L. N. Fang and Y. D. Li, *Energy & Fuels*, 2008, **22**, 1365–1370.
- 138 H. S. Roh, Y. Wang and D. L. King, *Topics in Catalysis*, 2008, **49**, 32–37.
- 139 E. C. Wanat, B. Suman and L. D. Schmidt, *J. Catal.*, 2005, **235**, 18–27.
- 140 J. R. Salge, G. A. Deluga and L. D. Schmidt, *J. Catal.*, 2005, **235**, 69–78.
- 141 L. O. O. Costa, S. M. R. Vasconcelos, A. L. Pinto, A. M. Silva, L. V. Mattos, F. B. Noronha and L. E. P. Borges, *Journal of Materials Science*, 2008, **43**, 440–449.
- 142 A. M. Silva, A. M. D. De Farias, L. O. O. Costa, A. Barandas, L. V. Mattos, M. A. Fraga and F. B. Noronha, *Appl. Catal. A-Gen.*, 2008, **334**, 179–186.
- 143 A. M. Silva, L. O. O. Costa, A. Barandas, L. E. P. Borges, L. V. Mattos and F. B. Noronha, *Catal. Today*, 2008, **133**, 755–761.
- 144 S. Cavallaro, V. Chiodo, A. Vita and S. Freni, *J. Power Sources*, 2003, **123**, 10–16.
- 145 G. A. Deluga, J. R. Salge, L. D. Schmidt and X. E. Verykios, *Science*, 2004, **303**, 993–997.
- 146 E. Vesselli, G. Comelli, R. Rosei, S. Freni, F. Frusteri and S. Cavallaro, *Appl. Catal. A-Gen.*, 2005, **281**, 139–147.
- 147 O. Akdim, W. J. Cai, V. Fierro, H. Provendier, A. Van Veen, W. J. Shen and C. Mirodatos, *Topics in Catalysis*, 2008, **51**, 22–38.
- 148 V. Fierro, O. Akdim, H. Provendier and C. Mirodatos, *J. Power Sources*, 2005, **145**, 659–666.
- 149 V. Fierro, O. Akdim and C. Mirodatos, *Green Chemistry*, 2003, **5**, 20–24.
- 150 V. Fierro, V. Klouz, O. Akdim and C. Mirodatos, *Catal. Today*, 2002, **75**, 141–144.

-
- 151 N. Hebben, C. Diehm and O. Deutschmann, *Appl. Catal. A-Gen.*, 2010, **388**, 225–231.
- 152 C. Diehm, T. Kaltschmitt and O. Deutschman, *Energy and Fuels*, 2012, submitted.
- 153 S. Cavallaro, V. Chiodo, S. Freni, N. Mondello and F. Frusteri, *Applied Catalysis A: General*, 2003, **249**, 119–128.
- 154 S. M. de Lima, R. C. Colman, G. Jacobs, B. H. Davis, K. R. Souza, A. F. F. de Lima, L. G. Appel, L. V. Mattos and F. B. Noronha, *Catalysis Today*, 2009, **146**, 110–123.
- 155 A. N. Fatsikostas, D. I. Kondarides and X. E. Verykios, *Catalysis Today*, 2002, **75**, 145–155.
- 156 K. L. Hohn and Y.-C. Lin, *ChemSusChem*, 2009, **2**, 927–940.
- 157 V. Kirillov, V. Meshcheryakov, V. Sobyenin, V. Belyaev, Y. Amosov, N. Kuzin and A. Bobrin, *Theoretical Foundations of Chemical Engineering*, 2008, **42**, 1–11.
- 158 D. K. Liguras, K. Goundani and X. E. Verykios, *Journal of Power Sources*, 2004, **130**, 30–37.
- 159 M. Ni, D. Y. C. Leung and M. K. H. Leung, *International Journal of Hydrogen Energy*, 2007, **32**, 3238–3247.
- 160 M. Nilsson, X. Karatzas, B. Lindström and L. J. Pettersson, *Chemical Engineering Journal*, 2008, **142**, 309–317.
- 161 K. Sato, K. Kawano, A. Ito, Y. Takita and K. Nagaoka, *ChemSusChem*, 2010, **3**, 1364–1366.